International Journal of
*Molecular Sciences*

MDPI

*Review*

# For the Better or for the Worse? The Effect of Manganese on the Activity of Eukaryotic DNA Polymerases

**Eva Balint and Ildiko Unk ***

Institute of Genetics, HUN-REN Biological Research Centre Szeged, H-6726 Szeged, Hungary; balint.eva@brc.hu
* Correspondence: unk.ildiko@brc.hu

**Abstract:** DNA polymerases constitute a versatile group of enzymes that not only perform the essential task of genome duplication but also participate in various genome maintenance pathways, such as base and nucleotide excision repair, non-homologous end-joining, homologous recombination, and translesion synthesis. Polymerases catalyze DNA synthesis via the stepwise addition of deoxynucleoside monophosphates to the 3′ primer end in a partially double-stranded DNA. They require divalent metal cations coordinated by active site residues of the polymerase. $Mg^{2+}$ is considered the likely physiological activator because of its high cellular concentration and ability to activate DNA polymerases universally. $Mn^{2+}$ can also activate the known DNA polymerases, but in most cases, it causes a significant decrease in fidelity and/or processivity. Hence, $Mn^{2+}$ has been considered mutagenic and irrelevant during normal cellular function. Intriguingly, a growing body of evidence indicates that $Mn^{2+}$ can positively influence some DNA polymerases by conferring translesion synthesis activity or altering the substrate specificity. Here, we review the relevant literature focusing on the impact of $Mn^{2+}$ on the biochemical activity of a selected set of polymerases, namely, Polβ, Polλ, and Polμ, of the X family, as well as Polι and Polη of the Y family of polymerases, where congruous data implicate the physiological relevance of $Mn^{2+}$ in the cellular function of these enzymes.

**Keywords:** DNA polymerases; manganese; translesion synthesis; catalytic activity; polymerase families



**Citation:** Balint, E.; Unk, I. For the Better or for the Worse? The Effect of Manganese on the Activity of Eukaryotic DNA Polymerases. *Int. J. Mol. Sci.* **2024**, *25*, 363. https://doi.org/10.3390/ijms25010363

Academic Editor: Maria Carmela Bonaccorsi Di Patti

Received: 8 December 2023
Revised: 22 December 2023
Accepted: 24 December 2023
Published: 27 December 2023



## 1. Eukaryotic DNA Polymerases

DNA polymerases can synthesize DNA in a template-dependent manner [1]. They act on a primer/template DNA substrate with a free hydroxyl group at the 3′ position of the sugar moiety of the last nucleotide in the primer. The 3′-OH group is the attachment site during polymerization that proceeds through the sequential addition of dNMPs in an order directed by the template strand. One fundamental cellular task requiring this activity is genome duplication during cell division. Nevertheless, DNA synthesis is needed for several other processes, like the different DNA repair pathways, such as base (BER) and nucleotide excision repair, homologous recombination, non-homologous end-joining (NHEJ), and translesion synthesis (TLS). The structure of the substrate DNA in these pathways varies considerably. Because of this and to fulfill their cellular roles, DNA polymerases became highly specialized [2–4]. For example, some DNA polymerases possess exonuclease activity that proofreads mistakes committed by the enzyme. Still, others do not, while some even exhibit 5′- deoxyribophosphate (dRP) lyase, endonuclease, or terminal transferase activities. The fidelity and processivity of polymerases can also differ substantially in accordance with their cellular tasks. The diverse group of eukaryotic DNA polymerases can be classified into four families based on the primary sequence homology of the catalytic domain [5]: the A family contains pols γ, θ, and ν; the B family contains α, δ, ε, and ζ; the Y family includes η, ι, κ, and Rev1; and the X family consists of Polβ, λ, μ, and TdT. Polymerases belonging to the same family share some features, but they all exhibit individual characteristics (Figure 1).

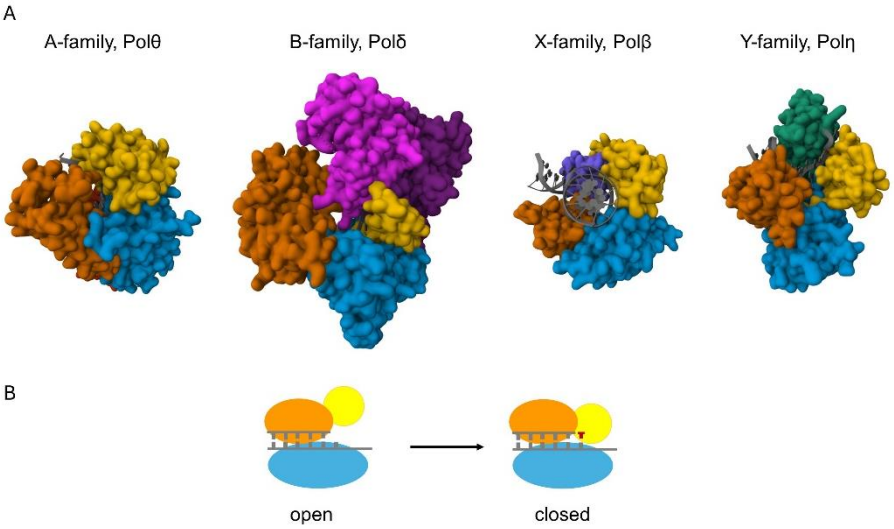


**Figure 1.** Structures of the catalytic cores of the eukaryotic DNA polymerases. (**A**) The proteins are shown in surface representation and the DNA helices are shown in cartoon representation (colored grey) [6]. The view in all the structures is down the DNA helix axis, except for Polβ, which introduces a 90° bend into the DNA. A family Pols, represented by human Polθ (4X0P) [7], possess palm (blue), fingers (yellow), thumb (orange), and exonuclease (red) domains. Exonuclease domain is positioned behind the palm and thumb domains in the figure. B family Pols, represented by yeast Polδ (3IAY) [8], have N-terminal (purple), exonuclease (magenta), palm (blue), fingers (yellow), and thumb (orange) domains. X family pols, such as human Polβ (4KLE) [9], employ palm, fingers, and thumb domains, as well as a 5′-dRP lyase domain (violet). Y family pols, represented by human Polη (3MR2) [10], have palm, fingers, and thumb domains, and possess a unique polymerase-associated domain (PAD) (green). (**B**) Schematic of the conformational change of high-fidelity polymerases. The pol binds the DNA in an "open" conformation; then, upon binding the incoming nucleotide, the finger domain (yellow) moves to a "closed" conformation that ensures correct base pairing.

### *1.1. B Family*

The B family members are multisubunit enzymes [11]. This group includes the main replicative polymerases Polε and Polδ. Their role is to carry out faithful duplication of the genomic DNA so that the inheriting material can be transferred to the next generation of cells unchanged. In accordance with this, they are the highest-fidelity DNA polymerases. The high fidelity is attributable to their active centers that impose strict geometric selection during synthesis so that the polymerases cannot accommodate modified, damaged bases and non-Watson–Crick base pairs. In addition, pols δ and ε exhibit a 3′–5′ exonuclease activity that removes accidental errors made by the polymerases, further lowering the error rate during synthesis. Polα is a primase that provides the primer for pols δ and ε, as it can start synthesis de novo on a template strand synthesizing a short 12–15 nt RNA primer by its primase subunit, which is extended with dNTPs by its polymerase subunit. Polα does not have exonuclease activity, and because of this, its fidelity is lowered. Polζ also lacks exonuclease activity. It stands out from the group because it does not work during normal replication. It comes into play when a mismatched or damaged base introduced by other polymerases must be extended. Because its extension activity is essential for synthesis across DNA lesions, Polζ is considered a translesion synthesis polymerase, together with the Y family polymerases.

### *1.2. Y Family*

Polymerases in the Y family are TLS polymerases [12]. They exhibit low fidelity on undamaged DNA due to their spacious, non-selective active center that can accommodate modified, damaged, or mismatched base pairs, in sharp contrast to replicative polymerases. Furthermore, they lack proofreading exonuclease activity. Surprisingly, they can support

faithful synthesis across DNA lesions called their cognate lesions, whereas they perform error-prone synthesis across many others. These error-prone polymerases are activated when replication stalls at a DNA lesion site where a TLS polymerase replaces the replicative polymerase to carry out a lesion bypass. Beyond lesion bypass, TLS polymerases must be strictly regulated to avoid the accumulation of excess mutations in the genome. The distributive nature of their synthetic activity supports this confinement. While Pols η and ι can insert nucleotidesacross various DNA lesions, in most cases, they cannot continue the synthesis beyond the inserted nucleotide. Meanwhile, Polκ can work as an inserter and an extender during TLS due to its ability to extend from damaged or mispaired primer ends. Rev1 is very limited as a polymerase: it can catalyze the efficient incorporation of cytosine in a templated manner, whereas it is highly inefficient at inserting other nucleotides. However, it plays an essential scaffolding role during TLS by binding other TLS polymerases.

### *1.3. X Family*

X family polymerases are small, gap-filling repair polymerases that function in the repair of short single-stranded DNA gaps during base excision repair, and in the direct joining of broken DNA ends with minimal or no homology during NHEJ and V(D)J recombination, which is a process that ensures immunoglobulin diversity [13]. In addition to the repair function, pols β, λ, and μ exhibit DNA lesion bypass activity. These polymerases do not have exonuclease activity, but Polβ and λ exhibit a dRP lyase activity that can remove 5′-deoxyribophosphate moieties generated by apurinic/apyrimidinic (AP) endonucleases during BER. Moreover, Polλ and μ were shown to exhibit terminal deoxynucleotidyl transferase activity, like TdT. While Polβ and λ show moderate fidelity, the error rate of Polμ is high, and TdT works primarily in a non-templated fashion and is only expressed in cells engaged in V(D)J recombination [14].

### *1.4. A Family*

The A family member Polγ is responsible for the faithful duplication of the mitochondrial genome, which is supported by its high fidelity and a 3′–5′ proofreading exonuclease activity. In addition, Polγ also has a 5′-dRP lyase activity that is important for its mitochondrial repair function and it shows limited TLS capacity. In contrast, Polθ and ν are low-fidelity enzymes that take part in translesion synthesis, microhomology-mediated end joining, and DNA cross-link repair [15]. Intriguingly, Polθ shows lyase activity and it contains a helicase domain, though helicase activity has not been detected for this protein. Polν is remarkably able to bypass bulky major groove DNA adducts.

## 2. Metal Ions in DNA Polymerization

All DNA polymerases catalyze the same chemical reaction for which they apply a very similar structural arrangement of the catalytic subunit resembling a human right hand. High-fidelity polymerases undergo a conformational change during catalysis when the right-hand structure transitions from an open to a closed state (Figure 1B) [16]. This conformational change contributes to the fidelity of DNA synthesis. Keeping the analogy, the catalytic subunit has palm, thumb, and finger domains (Figure 1A). The thumb domain binds the double-stranded DNA, the fingers capture the incoming dNTP and the single-stranded template strand, and the palm contains the amino acids that coordinate two divalent metal cations essential for the chemical reaction [17]. The two metals have distinct roles and occupy different positions in the active center [18]. One serves as the catalytic metal at the so-called A site, and the other is the nucleotide metal at the B site. The A site metal helps to lower the $pK_a$ of the 3′-OH proton at the primer terminus for nucleophilic attack on the α-phosphate of the incoming nucleotide. The B site metal coordinates the non-bridging oxygens of the triphosphate of the bound nucleotide and helps to neutralize the negative charge during the transition state. After a phosphodiester bond is newly formed between the 3′-O of the primer and the α-phosphate of the dNTP, a pyrophosphate is released. Several structural studies suggest the presence of a third metal during the

reaction, but the exact role of the third metal is still debated [19,20]. The identity of the metal cofactor utilized by a given enzyme in the cell is usually uncertain due to technical challenges. $Mg^{2+}$ has been considered the physiologically relevant activating metal for DNA polymerases because it is abundant in the cell and activates all known DNA polymerases in vitro. Early studies revealed that other metal ions can activate polymerases as well, but usually with much less efficiency and/or fidelity than $Mg^{2+}$. Moreover, the cellular concentrations of other bivalent metals are significantly lower compared with $Mg^{2+}$, supporting the pivotal role of $Mg^{2+}$ in DNA synthesis. Particularly, the intracellular $Mn^{2+}$ concentration is estimated to be in the μM range (up to 75 μM), whereas that of $Mg^{2+}$ spans over to the mM range (0.2–7 mM), though the concentration is dependent on the cell type, developmental stage, and organism [21–23].

*Mutagenic Effect of Manganese*

Like $Mg^{2+}$, $Mn^{2+}$ can activate all DNA polymerases. However, $Cd^{2+}$, $Co^{2+}$, $Ni^{2+}$, $Cr^{2+}$, and $Mn^{2+}$ have been classified as mutagens and potential carcinogens because they cause polymerases to make frequent errors during DNA synthesis in vitro [24–26]. $Mn^{2+}$ was shown to decrease the fidelity of viral, bacterial, and eukaryotic DNA polymerases. In the case of avian myeloblastosis virus DNA polymerase, the efficiency of DNA synthesis was half, and the misincorporation rate was twice or three times higher with $Mn^{2+}$ compared with $Mg^{2+}$, depending on the applied Mn concentration. Bacteriophage T4 DNA polymerase and *Escherichia coli* DNA polymerase I not only misincorporated with elevated rates but removed correctly paired nucleotides with higher rates than mispaired nucleotides if the reactions contained $Mn^{2+}$ instead of $Mg^{2+}$ [27]. The misinsertion capability of human DNA Polα was enhanced by $Mn^{2+}$ as well.

## 3. Manganese Empowering DNA Polymerases

Most of the aforementioned DNA polymerases exhibit high fidelity with $Mg^{2+}$ and are responsible for the duplication of viral, bacterial, or eukaryotic genomes. The reduced accuracy detected with $Mn^{2+}$ would cause detrimental effects on their cellular role. However, it is clear now that beyond the deleterious effects, $Mn^{2+}$ can improve the activity of other DNA polymerases working in DNA repair and translesion synthesis-related processes. $Mn^{2+}$ can increase the efficiency of synthesis and the TLS capacity or change the substrate specificity of the DNA pols, enabling them to overcome a broader spectrum of obstacles. The polymerases for which substantial evidence supports $Mn^{2+}$ in the catalytic activation are the X family members Polβ, Polλ, and Polμ, and Polι and Polη of the Y family. Below, we summarize the available data concerning the effects of $Mn^{2+}$ on the biochemical properties of these enzymes. For comprehensive biochemical and structural summaries, we advise reading the excellent reviews published in recent years [2,3,12].

### 3.1. Polβ

Polβ is the smallest and probably the most studied eukaryotic DNA polymerase [28]. It can work on primed DNA, but its preferred substrate is a few-nucleotide gap-containing DNA where the enzyme binds both sides of the gap [29]. Polβ is considered the primary polymerase in the repair of abasic sites in BER [30]. AP sites are non-coding and, therefore, potentially mutagenic. They can arise via spontaneous hydrolysis or the action of glycosylases on modified bases. Over 10,000 AP sites are formed spontaneously in a mammalian cell in one day. Polβ catalyzes two steps of the repair where first a glycosylase removes the damaged base, leaving an AP site [31]. An AP-endonuclease makes a single-strand incision on the 5′-side of the AP site. Following this, Polβ performs high-fidelity gap-filling via its polymerase activity, using the 3′-OH at the nick, and then it removes the 5′-sugar-phosphate residues left behind by the AP endonuclease, using its 5′-dRP lyase activity. Finally, the remaining nick is sealed by a DNA ligase. Both the 5′-dRP lyase and polymerase activities are important for genomic integrity, as cancer-associated mutations exclusively affecting either the polymerase or the lyase domain were identified [28,32,33].

Moreover, Polβ is mutated in ~30% of human tumors, and disruption of the *POLB* gene coding for Polβ in mice results in embryonic lethality, which emphasizes the important role of the enzyme in maintaining genome stability [34–36]. During catalysis, the active center of the polymerase imposes strict geometric selection and undergoes an open-to-closed conformational transition, just like replicative polymerases [29]. This ensures accuracy, which is needed during the repair of the huge number of AP sites to preserve genome integrity. However, the fidelity is decreased compared with replicases due to the lack of intrinsic proofreading exonuclease activity. This, in turn, is advantageous for the lesion bypass activity of Polβ that is proposed to occur during gap-filling, ensuring fast repair, even in the presence of DNA lesions. 8-oxoguanine (8-oxoG), which is the major oxidative lesion [37,38], O6-methylguanine (O6mG), which is a highly mutagenic methylated lesion [39,40], N7-methylguanine (N7mG), which is the prevalent methylated lesion [41], AP-sites [42], and platinum adducts formed during chemotherapy [43–46] were shown to be bypassed by Polβ in vitro in an error-free or mutagenic manner.

Several bivalent metals, like $Co^{2+}$, $Fe^{2+}$, and $Zn^{2+}$, can serve as catalysts for Polβ, but the enzyme shows the highest activity with $Mg^{2+}$ and $Mn^{2+}$. A wide range (0.1–10 mM) of $Mg^{2+}$ and $Mn^{2+}$ concentrations support catalysis without a significant loss in activity [47], though a modest decrease in fidelity is observed in the presence of $Mn^{2+}$ (Table 1) [48–50]. Polβ even exhibited terminal transferase activity with Mn in crystals, which was not observed with $Mg^{2+}$ [51]. $Mn^{2+}$ significantly increased the bypass across an AP-site analog 3-hydroxy-2-hydroxymetylthetrahydrofuran [52]. The enzyme promoted mainly error-free synthesis opposite the major platinum adduct cisplatin-1,2-d(GpG) intramolecular crosslink with $Mn^{2+}$ by inserting two Cs opposite the two Gs of the lesion. The misinsertion of dTMP and dATP was 100-fold less efficient [53]. $Mn^{2+}$ enhanced the correct lesion bypass by eightfold through a fourfold decrease in the Michaelis–Menten constant ($K_m$), showing the affinity of the enzyme to the substrate, and a twofold increase in the velocity of the reaction ($k_{cat}$) [54]. Similarly, Polβ could catalyze the accurate bypass across an N7mG analog 2′-fluoro-m7dG in a gapped substrate with $Mg^{2+}$ via inserting the correct C, and no misinsertion was observed with T, even with $Mn^{2+}$ [41]. During the bypass of O6mG with $Mg^{2+}$, Polβ inserted the incorrect T with almost 20-fold higher efficiency than C opposite the lesion [40,54,55]. Using $Mn^{2+}$, the efficiency of misincorporation became 10-fold higher due to increased velocity, whereas the insertion efficiency of the correct C was twofold higher compared with $Mn^{2+}$, resulting in lowered fidelity [55]. Polβ could synthesize across thymin glycol, which is the most common oxidation product of thymine, using all four dNTPs in the presence of $Mg^{2+}$, inserting the correct A 10–100-fold more efficiently than an incorrect nucleotide [56]. $Mn^{2+}$ enhanced error-free insertion but also the misinsertion of non-complementary nucleotides, mainly through a 100-fold decrease in $K_m$. Based on the above examples, it seems that $Mn^{2+}$ does not alter the nucleotide preference of Polβ but it makes the enzyme more active and the bypass more efficient. Even though the enhancement is modest in most cases, it can have a significant impact since lesion bypassing by Polβ is highly inefficient with $Mg^{2+}$. For example, Polη bypasses platinum adducts with 40% efficiency, whereas Polβ with 2% efficiency of the synthesis on the unmodified template, and the synthesis opposite O6mG is 100-fold less efficient and across 2′-fluoro-m7dG is 300-fold less efficient than on undamaged DNA [40,41,44,57].

**Table 1.** Comparison of the effect of $Mg^{2+}$ and $Mn^{2+}$ on the catalytic activity and fidelity of Polβ.

| Substrate, Templating Nucleotide | Incoming Nucleotide | Cation | Velocity Constant | Affinity Constant | Efficiency | Magnitude of Stimulation, $Mn^{2+}/Mg^{2+}$ [a] | Misinsertion Frequency [b] | Reference |
|---|---|---|---|---|---|---|---|---|
| | | | $k_{cat}$ ($10^{-3}$ $s^{-1}$) [c] | $K_m$ (μM) [c] | $k_{cat}/K_m$ ($10^{-3}$ $s^{-1}$ $\mu M^{-1}$) | | | |
| 1 nt gapped DNA, G | dCTP | 5 mM $Mg^{2+}$ | 212.0 ± 19.9 | 0.6 ± 0.1 | 353.3 | 1 | 1 | [48] |
| | dCTP | 5 mM $Mn^{2+}$ | 30.3 ± 1.5 | 0.08 ± 0.01 | 383.7 | 1.08 | 1 | |
| | dTTP | 5 mM $Mg^{2+}$ | 2.8 ± 0.4 | 56.1 ± 4.6 | 0.049 | 1 | $1.4 \times 10^{-4}$ | |
| | dTTP | 5 mM $Mn^{2+}$ | 19.1 ± 0.8 | 11.2 ± 0.5 | 1.71 | 34 | $4.5 \times 10^{-3}$ | |

**Table 1.** *Cont.*

| Substrate, Templating Nucleotide | Incoming Nucleotide | Cation | Velocity Constant | Affinity Constant | Efficiency | Magnitude of Stimulation, $Mn^{2+}/Mg^{2+}$ [a] | Misinsertion Frequency [b] | Reference |
|---|---|---|---|---|---|---|---|---|
| 1 nt gapped DNA, $O^6$MedG | dCTP | 5 mM $Mg^{2+}$ | 14.5 ± 1.2 | 234.2 ± 24.5 | 0.062 | 1 | 1 | [55] |
| | dCTP | 5 mM $Mn^{2+}$ | 20.4 ± 1.6 | 193.3 ± 7.6 | 0.11 | 1.7 | 1 | |
| | dTTP | 5 mM $Mg^{2+}$ | 62.4 ± 11.0 | 56.2 ± 4.7 | 1.1 | 1 | 17 | |
| | dTTP | 5 mM $Mn^{2+}$ | 431.8 ± 53.2 | 38.7 ± 4.1 | 11.2 | 10 | 100 | |
| 1 nt gapped DNA, Pt-GG | dCTP | 5 mM $Mg^{2+}$ | 15.76 ± 1.24 | 5.22 ± 1.01 | 3.0 | 1 | | [54] |
| | dCTP | 5 mM $Mn^{2+}$ | 27.60 ± 1.62 | 1.14 ± 0.05 | 24.2 | 8 | | |
| | | | $k_{cat}$ ($s^{-1}$) | $K_m$ (μM) | $k_{cat}/K_m$ ($\mu M^{-1}$ $s^{-1}$) | | | |
| 5 nt gapped DNA, T | dATP | 1 mM $Mg^{2+}$ | 0.084 | 0.019 | 4.4 | 1 | | [56] |
| | dATP | 1 mM $Mn^{2+}$ | 0.078 | 0.085 | 0.92 | 0.2 | | |
| 5 nt gapped DNA, Thymine glycol | dATP | 1 mM $Mg^{2+}$ | 0.038 | 11.3 | 0.0034 | 1 | 1 | |
| | dATP | 1 mM $Mn^{2+}$ | 0.084 | 0.07 | 1.2 | 360 | 1 | |
| | dGTP | 1 mM $Mg^{2+}$ | 0.0064 | 12.5 | 0.0005 | 1 | $1.5 \times 10^{-1}$ | |
| | dGTP | 1 mM $Mn^{2+}$ | 0.064 | 3.51 | 0.018 | 36 | $1.5 \times 10^{-2}$ | |
| 2 nt gapped DNA, Thymine glycol | dATP | 1 mM $Mg^{2+}$ | 0.068 | 0.322 | 0.21 | 1 | 1 | |
| | dATP | 1 mM $Mn^{2+}$ | 0.093 | 0.043 | 2.2 | 10 | 1 | |
| | dGTP | 1 mM $Mg^{2+}$ | 0.0073 | 0.162 | 0.045 | 1 | $2.1 \times 10^{-1}$ | |
| | dGTP | 1 mM $Mn^{2+}$ | 0.083 | 0.653 | 0.13 | 2.8 | $6 \times 10^{-2}$ | |
| 1 nt gapped DNA, Thymine glycol | dATP | 1 mM $Mg^{2+}$ | 0.090 | 0.371 | 0.24 | 1 | 1 | |
| | dATP | 1 mM $Mn^{2+}$ | 0.092 | 0.006 | 15 | 63 | 1 | |
| | dGTP | 1 mM $Mg^{2+}$ | 0.070 | 61.73 | 0.0011 | 1 | $4.7 \times 10^{-3}$ | |
| | dGTP | 1 mM $Mn^{2+}$ | 0.076 | 0.337 | 0.23 | 200 | $1.4 \times 10^{-2}$ | |

[a] Magnitude of stimulation by Manganese was calculated as relative efficiency: $f_{rel} = (k_{cat}/K_m)_{Mn^{2+}}/(k_{cat}/K_m)_{Mg^{2+}}$. [b] Misinsertion frequency was calculated as relative efficiency: $f_{rel} = (k_{cat}/K_m)_{incorrect}/(k_{cat}/K_m)_{correct}$. [c] Steady-state kinetics: $k_{cat}$ is the turnover rate of the enzyme and $K_m$ is the Michaelis–Menten constant. Rows showing data measured in the presence of $Mn^{2+}$ have a blue background.

### 3.2. Polλ

Polλ exhibits all the catalytic activities possessed by other members of the X family [58,59]. It has polymerase, terminal transferase, polynucleotide synthetase, and 5′-dRP lyase, but lacks exonuclease activity [60–62]. It exhibits a 34% similarity of the catalytic domain with Polβ at the amino acid level. Despite this, the catalytic domain of Polλ does not undergo a large open-to-closed conformation change during catalysis, as opposed to Polβ [63]. Rather, it stays in a conformation resembling the closed state, even without substrate binding. The lack of a substrate-binding induced large conformational shift of the catalytic domain contributes to the lowered selectivity of the active center of Polλ compared with Polβ. It can even accommodate large G:G mispairs [64]. Polλ misinserts nucleotides during synthesis with a ~10-fold lower fidelity than Polβ, partly due to its ability to prebind nucleotides, even in the absence of DNA [65]. It generates single base deletions at a high rate caused by primer/template misalignment [66]. Synthesis by Polλ is distributive on a template/primer substrate but processive during the filling of short gaps [67]. These features suggest a more versatile role for Polλ compared with Polβ. Utilizing its activities, Polλ participates in BER, NHEJ, and V(D)J recombination. In BER, it can substitute for Polβ, and in NHEJ and V(D)J recombination, Polλ can fill the small gaps generated by the alignment of broken DNA ends having at least one base pair microhomology [68–71]. During gap filling, Polλ can perform translesion synthesis by inserting across lesions and it can extend from damaged DNA ends. The enzyme was shown to promote the error-prone bypass of AP sites [72], as well as the error-free bypass of 8-oxoG by preferentially extending the correct nucleotide opposite the lesion [73–75], 2-hydroxy adenine [76], (6-4)TT photoproducts [77], and N1-methyl-deoxyadenosine [78].

Interestingly, Polλ prefers $Mn^{2+}$ as a catalytic cofactor in in vitro experiments. It showed a threefold higher activity on a primer/template at a close-to-physiological (lower than 1 mM) $Mn^{2+}$ concentration but was inhibited at physiological (above 2 mM) $Mg^{2+}$ concentrations (Table 2) [47]. In contrast, Polα and Polδ were still active at 10–30 mM $Mg^{2+}$

and inhibited at 1 mM or higher $Mn^{2+}$. On primer/template substrates insertions of the correct and incorrect dNMPs were 1.5- and 5-fold more efficient with $Mn^{2+}$, respectively, yielding a slight decrease in fidelity [79]. Polλ inserted rNMPs into a primer/template with 100–200-fold less efficiency than dNMPs with $Mg^{2+}$, and this activity was increased 5–25-fold with $Mn^{2+}$. As opposed to a primer/template, $Mn^{2+}$ conferred a 100-fold increase in activity on a gapped DNA representing the cognate substrate of Polλ in the cell [56]. Polλ also showed higher TLS capacity in the presence of $Mn^{2+}$ as the error-free bypass of a thymine glycol in gapped substrates was 30-fold, and the misinsertion of dGMP was 60-fold more efficient compared with $Mg^{2+}$, resulting in a mere twofold decrease in fidelity [56]. $Mn^{2+}$ enabled Polλ to bypass an AP site [52]. The available data are too scarce to draw a definite conclusion, but the results show that similarly to Polβ, $Mn^{2+}$ elevates the activity of Polλ on a gapped substrate, damaged or undamaged, without compromising the insertion preference of the enzyme.

**Table 2.** Comparison of the effect of $Mg^{2+}$ and $Mn^{2+}$ on the catalytic activity and fidelity of Polλ.

| Substrate (Primer/Template), Templating Nucleotide | Incoming Nucleotide | Cation | Velocity Constant | Affinity Constant | Efficiency | Magnitude of Stimulation, $Mn^{2+}/Mg^{2+}$ [a] | Misinsertion Frequency [b] | Reference |
|---|---|---|---|---|---|---|---|---|
| | | | $k_{cat}$ ($s^{-1}$) [c] | $K_m$ (μM) [c] | $k_{cat}/K_m$ ($s^{-1}$ $M^{-1}$) [c] | | | |
| oligo(dT)/poly(dA), A | dTTP | 1 mM $Mg^{2+}$ | 0.006 | 4.7 | $1.2 \times 10^3$ | 1 | | [47] |
| | dTTP | 1 mM $Mn^{2+}$ | 0.016 | 3.2 | $5 \times 10^3$ | 4 | | |
| | | | $k_{cat}$ ($min^{-1}$) [d] | $K_d$ (μM) [d] | $k_{cat}/K_d$ ($min^{-1}$ $mM^{-1}$) [b] | | | |
| 19/40-mer, T | dATP | 1 mM $Mg^{2+}$ | 0.05 ± 0.01 | 0.8 ± 0.1 | 0.0625 ± 0.01 | 1 | 1 | [79] |
| | dATP | 0.1 mM $Mn^{2+}$ | 0.12 ± 0.02 | 1.2 ± 0.1 | 0.1 ± 0.05 | 1.6 | 1 | |
| | dCTP | 1 mM $Mg^{2+}$ | 0.002 ± 0.0005 | 4.5 ± 0.5 | 0.0004 ± 0.0001 | 1 | $6.4 \times 10^{-3}$ | |
| | dCTP | 0.1 mM $Mn^{2+}$ | 0.01 ± 0.003 | 4.5 ± 0.5 | 0.0022 ± 0.0002 | 5.5 | $2.2 \times 10^{-2}$ | |
| | dGTP | 1 mM $Mg^{2+}$ | 0.008 ± 0.004 | 3 ± 0.3 | 0.002 ± 0.0003 | 1 | $3.2 \times 10^{-2}$ | |
| | dGTP | 0.1 mM $Mn^{2+}$ | 0.02 ± 0.01 | 2.5 ± 0.2 | 0.008 ± 0.01 | 4 | $8.0 \times 10^{-2}$ | |
| | ATP | 1 mM $Mg^{2+}$ | 0.01 ± 0.002 | 12 ± 2 | 0.0008 ± 0.0001 | 1 | $1.3 \times 10^{-2}$ | |
| | ATP | 0.1 mM $Mn^{2+}$ | 0.015 ± 0.005 | 3.7 ± 2 | 0.004 ± 0.001 | 5 | $4.0 \times 10^{-2}$ | |
| 20/40-mer, G | dCTP | 1 mM $Mg^{2+}$ | 0.2 ± 0.08 | 0.9 ± 0.1 | 0.22 ± 0.03 | 1 | 1 | [79] |
| | dCTP | 0.1 mM $Mn^{2+}$ | 0.5 ± 0.2 | 1.5 ± 0.1 | 0.33 ± 0.04 | 1.5 | 1 | |
| | dGTP | 1 mM $Mg^{2+}$ | 0.004 ± 0.001 | 0.8 ± 0.2 | 0.005 ± 0.001 | 1 | $2.3 \times 10^{-2}$ | |
| | dGTP | 0.1 mM $Mn^{2+}$ | 0.04 ± 0.003 | 1.4 ± 0.1 | 0.028 ± 0.006 | 5.6 | $8.5 \times 10^{-2}$ | |
| | CTP | 1 mM $Mg^{2+}$ | 0.01 ± 0.003 | 9 ± 2 | 0.0011 ± 0.0002 | 1 | $5 \times 10^{-3}$ | |
| | CTP | 0.1 mM $Mn^{2+}$ | 0.08 ± 0.01 | 2.7 ± 0.5 | 0.029 ± 0.004 | 26 | $8.8 \times 10^{-3}$ | |
| 21/40-mer, C | dGTP | 1 mM $Mg^{2+}$ | 0.08 ± 0.01 | 3 ± 0.4 | 0.026 ± 0.002 | 1 | 1 | [79] |
| | dGTP | 0.1 mM $Mn^{2+}$ | 0.2 ± 0.03 | 2.5 ± 0.2 | 0.08 ± 0.02 | 3 | 1 | |
| | GTP | 1 mM $Mg^{2+}$ | 0.003 ± 0.001 | 10 ± 1 | 0.0003 ± 0.0001 | 1 | $1.1 \times 10^{-2}$ | |
| | GTP | 0.1 mM $Mn^{2+}$ | 0.03 ± 0.01 | 6.5 ± 0.7 | 0.0046 ± 0.001 | 15 | $5.8 \times 10^{-2}$ | |
| | | | $k_{cat}$ ($s^{-1}$) [c] | $K_m$ (μM) [c] | $k_{cat}/K_m$ (μ$M^{-1}$ $s^{-1}$) | | | |
| 5 nt gapped DNA, T | dATP | $Mg^{2+}$ | 0.026 | 6.44 | 0.0041 | 1 | | [56] |
| | dATP | $Mn^{2+}$ | 0.060 | 0.144 | 0.42 | 100 | | |
| 2 nt gapped DNA, Thymineglycol | dATP | $Mg^{2+}$ | 0.006 | 0.091 | 0.069 | 1 | 1 | |
| | dATP | $Mn^{2+}$ | 0.027 | 0.012 | 2.3 | 34 | 1 | |
| | dGTP | $Mg^{2+}$ | 0.011 | 1.42 | 0.008 | 1 | $1.2 \times 10^{-1}$ | |
| | dGTP | $Mn^{2+}$ | 0.043 | 0.083 | 0.52 | 67 | $2.3 \times 10^{-1}$ | |

[a] Magnitude of stimulaton by Manganese was calculated as relative efficiency: $f_{rel} = (k_{cat}/K_m)_{Mn^{2+}}/(k_{cat}/K_m)_{Mg^{2+}}$. [b] Misinsertion frequency was calculated as relative efficiency: $f_{rel} = (k_{cat}/K_m)_{incorrect}/(k_{cat}/K_m)_{correct}$. [c] Steady-state kinetics: kcat is the turnover rate of the enzyme and $K_m$ is the Michaelis–Menten constant. [d] Pre-steady-state kinetics: $k_{pol}$ is the maximum rate constant of the pre-steady-state burst phase and $K_d$ is the dissociation constant of the Pol–DNA–dNTP complex. Rows showing data measured in the presence of $Mn^{2+}$ have a blue background.

### 3.3. Polμ

Polμ is a low-fidelity, distributive polymerase that functions in NHEJ and the V(D)J recombination [71,80–83]. The enzyme shares 41% identity with TdT at the amino acid level and besides the template-dependent polymerase activity, it exhibits template-independent terminal transferase activity [84]. It possesses several surprising features not found with other polymerases. It is a versatile enzyme that can act on various substrates in vitro, like gap-containing templates, unpaired primers, or overhanging primers [71]. Moreover, Polμ stands out from the other polymerases by having the ability to align broken DNA ends that have no complementarity at all. Its terminal transferase activity, which involves extending single-stranded DNA, was proposed to be required for creating or increasing the complementarity of broken DNA ends [85]. During the repair of small gaps, Polμ can realign the primer/template so that it skips the first templating nucleotide and uses the nucleotide adjacent to the 5′ side of the gap instead as a template generating a few nucleotide deletions with high frequency [86,87]. The enzyme remains rigid throughout the catalytic cycle without showing even the small dNTP-binding-induced movements of active site side chains characteristic of Polλ [88]. This rigidity is probably required to firmly engage the often unstable DNA substrates of NHEJ. During template-dependent synthesis, Polμ can utilize both dNTPs and rNTPs with almost the same efficiency [89–91]. It discriminates between rNTPs and dNTPs with a 1000-fold lower efficiency than Polβ, showing a mere 10-fold or lower preference toward dNTPs. In addition, Polμ exhibits lesion bypass activity opposite several DNA lesions. It bypasses most of the lesions, such as AP-site, 8-oxoG, platinum adducts, and other bulky lesions, in an error-prone way by realigning the primer/template [92–94]. Surprisingly, during the bypass of the UV-induced TT dimer, Polμ primarily inserts the two correct As opposite the lesion [92].

Like its siblings in the X family, Polμ is more active with $Mn^{2+}$ compared with $Mg^{2+}$ [84]. $Mn^{2+}$ was suggested to be the in vivo metal co-factor of Polμ since it promoted efficient insertion of only the correct nucleotide at physiological concentrations (10–40 μM), whereas a high concentration (1 mM) compromised the fidelity of Polμ on various gapped substrates [95]. Fidelity was further increased when rNTPs were added instead of ddNTPs. Although the kinetic parameters were not determined, a similar amount of insertion products were obtained using 100-fold lower concentrations of ddNTPs or rNTPs in the presence of $Mn^{2+}$ versus $Mg^{2+}$. When physiological concentrations of nucleotides were provided, an up to 30-fold shorter time was needed to obtain the same amount of insertion product with $Mn^{2+}$ compared with $Mg^{2+}$. Polμ could also extend RNA primers with rNTPs and $Mn^{2+}$ strongly improved the incorporation [89]. Single-turnover kinetic analysis and time-lapse X-ray crystallography using a gapped substrate and dNTPs showed that the overall insertion efficiency ($k_{pol}/K_d$) was 50-fold higher in the presence of $Mn^{2+}$ versus $Mg^{2+}$. This increase resulted mostly from the enhanced velocity, as the rate constant ($k_{pol}$) of Polμ was 13.5 fold higher, while the $K_d$ for the templated correct incoming dNTP was only 3.5-fold lower (Table 3) [96]. $Mn^{2+}$ enhanced the incorporation of both 8-oxo-dGTP and 8-oxo-rGTP into a gapped substrate [97,98].

**Table 3.** Comparison of the effects of $Mg^{2+}$ and $Mn^{2+}$ on the catalytic activity and fidelity of Polμ.

| Substrate, Templating Nucleotide | Incoming Nucleotide | Cation | Velocity Constant | Affinity Constant | Efficiency | Magnitude of Stimulation, $Mn^{2+}/Mg^{2+}$ [a] | Misinsertion Frequency [b] | Reference |
|---|---|---|---|---|---|---|---|---|
| 1 nt gapped DNA, A | | | $k_{pol}$ ($s^{-1}$) [d] | $K_d$ (μM) [d] | $k_{pol}/K_d$ ($\mu M^{-1}$ $s^{-1}$) [c] | | | |
| | dTTP | 10 mM $Mg^{2+}$ | 6.0 ± 0.2 | 192 ± 21 | 0.031 ± 0.004 | 1 | | [96] |
| | dTTP | 1 mM $Mn^{2+}$ | 81 ± 7 | 54 ± 18 | 1.5 ± 0.5 | 48 | | |
| | | | $k_{cat}$ ($min^{-1}$) [c] | $K_m$ (μM) [c] | $k_{cat}/K_m$ ($min^{-1}$ $\mu M^{-1}$) | | | |
| 1 nt gapped DNA, C | dGTP | 10 mM $Mg^{2+}$ | 5.70 ± 0.21 | 3.48 ± 0.31 | 1.64 ± 0.16 | 1 | 1 | |
| | dGTP | 1 mM $Mn^{2+}$ | 0.16 ± 0.01 | 0.006 ± 0.001 | 26.9 ± 4.7 | 16 | 1 | [98] |
| 1 nt gapped DNA, A | dGTP | 10 mM $Mg^{2+}$ | 0.04 ± 0.01 | 55.6 ± 5.9 | 0.0007 ± 0.0002 | 1 | $4.3 \times 10^{-4}$ [e] | |
| | dGTP | 1 mM $Mn^{2+}$ | 2.98 ± 0.01 | 21.3 ± 2.3 | 0.14 ± 0.02 | 200 | $5.2 \times 10^{-3}$ [e] | |

**Table 3.** *Cont.*

| Substrate, Templating Nucleotide | Incoming Nucleotide | Cation | Velocity Constant | Affinity Constant | Efficiency | Magnitude of Stimulation, $Mn^{2+}/Mg^{2+}$ [a] | Misinsertion Frequency [b] | Reference |
|---|---|---|---|---|---|---|---|---|
| | | | $k_{cat}$ ($10^{-3}$ $min^{-1}$) [c] | $K_m$ (μM) [c] | $k_{cat}/K_m$ ($min^{-1}$ $\mu M^{-1}$) | | | |
| 1 nt gapped DNA, T | dATP | 10 mM $Mg^{2+}$ | 236.2 ± 5.3 | 3.1 ± 0.3 | $76.6 \times 10^{-3}$ | | | [99] |
| | dGTP | 10 mM $Mg^{2+}$ | 28.3 ± 0.6 | 5.7 ± 0.5 | $4.9 \times 10^{-3}$ | 1 | $6.4 \times 10^{-2}$ | |
| | dGTP | 10 mM $Mn^{2+}$ | 100.1 ± 2.6 | 5.2 ± 0.6 | $19.2 \times 10^{-3}$ | 3.9 | n.d. | |

[a] Magnitude of stimulaton by Manganese was calculated as relative efficiency: $f_{rel} = (k_{cat}/K_m)_{Mn^{2+}}/(k_{cat}/K_m)_{Mg^{2+}}$. [b] Misinsertion frequency was calculated as relative efficiency: $f_{rel} = (k_{cat}/K_m)_{incorrect}/(k_{cat}/K_m)_{correct}$. [c] Steady-state kinetics: $k_{cat}$ is the turnover rate of the enzyme and $K_m$ is the Michaelis–Menten constant. [d] Pre-steady-state kinetics: $k_{pol}$ is the maximum rate constant of the pre-steady-state burst phase and $K_d$ is the dissociation constant of the Pol–DNA–dNTP complex. [e] Unconventionally, here, the same incoming nucleotide was compared opposite different templating bases. Rows showing data measured in the presence of $Mn^{2+}$ have a blue background.

Like Polλ, Polμ can prebind the nucleotide before binding the template DNA [51,100]. In the presence of $Mg^{2+}$, Polμ prebinds dNTPs or rNTPs with low affinity, with $K_d$ values in the range of 98−236 μM, as opposed to $Mn^{2+}$, which promotes much stronger prebinding with $K_d$ values in the range of 0.22−2.76 μM. Although nucleotide prebinding before binding the DNA template causes infidelity, it can be very advantageous for creative, non-templated synthesis. Based on its preference in vitro, it was proposed that rNTPs and $Mn^{2+}$ are the physiological substrates of Polμ during NHEJ. Indeed, 65% of cellular NHEJ products contained transiently embedded rNTPs, which was dependent on Polμ [101]. Additionally, NHEJ reconstitution experiments with Polμ showed that $Mn^{2+}$ and rNTP insertion stimulated the coupled ligation of the broken DNA strands, whereas, with $Mg^{2+}$ and dNTPs, the ligation step was inefficient [102].

### *3.4. Polι*

Polι belongs to the Y family of TLS polymerases, which rescue stalled replication forks by synthesizing across DNA lesions or bypassing DNA damage during postreplication repair [103]. Uniquely among TLS polymerases, Polι has an additional 5′-dRP lyase activity through which it can participate in BER [104]. It is a very distributive and error-prone polymerase; however, its infidelity is strongly sequence-dependent and may differ by 100,000-fold [105–107]. Polι is the most accurate opposite template A; it is less accurate opposite templates G or C; while fidelity is completely lost opposite template T, where Polι favors the incorporation of a wrong G instead of the correct A. The crystal structure of the catalytic domain revealed that unlike other polymerases, Polι binds the template base in a flipped "syn" conformation instead of the usual "anti" conformation because of its narrow active site [108]. This results in the formation of Hoogsteen hydrogen bonds with the incoming nucleotide instead of Watson–Crick base pairing. Moreover, in the case of template T, Polι may induce wobble base pairing with the incoming nucleotide [109]. This versatility of Polι enables the enzyme to efficiently bypass various types of DNA damage, like AP-sites, 8-oxoG, CPD, 6–4 photoproducts, and methyl adducts [110–115].

Polι exhibited the greatest activity in the presence of $Mn^{2+}$ in in vitro primer extension experiments [116]. The enzyme showed the highest activity in low, close-to-physiological concentrations of $Mn^{2+}$ (50–250 μM) and low levels of $Mg^{2+}$ (100–500 μM), whereas $Mg^{2+}$ concentrations higher than 2 mM had a strong inhibitory effect. The enzyme preferred $Mn^{2+}$, even in a 40-fold excess of $Mg^{2+}$. Steady-state kinetics analysis showed that Polι was 30–6000-fold more active in the presence of 75 μM $Mn^{2+}$ than in the presence of 5 mM $Mg^{2+}$ (Table 4). The increase was the result of a huge decrease in $K_m$, while the $v_{max}$ values were virtually unchanged. When applying low 250 μM $Mg^{2+}$, the change was less dramatic. However, interesting individual differences were observed on various templates. Opposite template T, the $K_m$ value for the correct incorporation of A decreased by 10-fold, while for the incorrect G, it decreased fivefold in the presence of low $Mn^{2+}$ versus low $Mg^{2+}$. This led to an increase in the fidelity of the enzyme now favoring the incorporation of the correct A

by twofold instead of the incorrect G. In contrast, on template A, the $K_m$ value decreased by 30-fold for the correct incorporation of T and 23,000-fold for the incorrect A when using $Mn^{2+}$ versus $Mg^{2+}$. This resulted in a steep fall in fidelity with the preference for correct T dropping from 4000-fold to 13-fold. Thus, $Mn^{2+}$ increased the polymerization activity of Polι on both templates but it increased the fidelity on template T while decreasing it on template A. Polι could incorporate rNTPs during primer extension with $Mn^{2+}$ [117]. Its poor base selectivity observed for dNTPs was improved when using rNTPs. Furthermore, $Mn^{2+}$ enhanced the DNA damage bypass ability of Polι opposite several lesions such as CPD, 6–4 photoproduct, BPDE, AP-site, and N2-ethylamine [116,118]. In summary, $Mn^{2+}$ improved the catalytic efficiency of Polι on undamaged DNA, concomitantly altering its nucleotide preference, and hence the fidelity of the enzyme, and it increased the efficiency of TLS as well. The relevance of its strange biochemical characteristics and the exact function of Polι are still enigmatic. It was proposed to take part in the somatic hypermutation of immunoglobulin genes, but unambiguous in vivo data are still lacking [119–122]. On the other hand, the role of Polι in the cellular response to different DNA-damaging agents is supported by several studies [115,123,124]. It contributed to the UV resistance and UV-induced mutagenesis of human cells and the mutagenic replication through the anticancer nucleoside cytarabine.

**Table 4.** Comparison of the effect of $Mg^{2+}$ and $Mn^{2+}$ on the catalytic activity and fidelity of Polι.

| Substrate (Primer/Template), Templating Nucleotide | Incoming Nucleotide | Cation | Velocity Constant | Affinity Constant | Efficiency | Magnitude of Stimulation, $Mn^{2+}/Mg^{2+}$ [a] | Misinsertion Frequency [b] | Reference |
|---|---|---|---|---|---|---|---|---|
| | | | $V_{max}$ (% $min^{-1}$) [c] | $K_m$ (μM) [c] | $V_{max}/K_m$ (% $min^{-1}$ $\mu M^{-1}$) | | | |
| 16/48-mer, T | dATP | 5 mM $Mg^{2+}$ | 5 ± 0.8 | 2.7 ± 0.5 | 1.85 | 1 | 1 | [116] |
| | dATP | 0.075 mM $Mn^{2+}$ | 7.1 ± 0.5 | 0.0011 ± 0.0002 | 6450 | 3486 | 1 | |
| | dGTP | 5 mM $Mg^{2+}$ | 8.3 ± 0.9 | 1.8 ± 0.3 | 4.6 | 1 | 2.5 | |
| | dGTP | 0.075 mM $Mn^{2+}$ | 6.3 ± 1 | 0.0022 ± 0.0003 | 2860 | 622 | $4.4 \times 10^{-1}$ | |
| 20/50-mer, A | dTTP | 5 mM $Mg^{2+}$ | 10 ± 2 | 0.06 ± 0.01 | 167 | 1 | 1 | |
| | dTTP | 0.075 mM $Mn^{2+}$ | 2.6 ± 0.5 | 0.00053 ± 0.0001 | 4900 | 30 | 1 | |
| | dATP | 5 mM $Mg^{2+}$ | 5 ± 1.1 | 90 ± 17 | 0.06 | 1 | $3.6 \times 10^{-4}$ | |
| | dATP | 0.075 mM $Mn^{2+}$ | 1.1 ± 0.3 | 0.003 ± 0.0008 | 370 | 6600 | $7.5 \times 10^{-2}$ | |
| | | | $k_{cat}$ ($min^{-1}$) [c] | $K_m$ (μM)[c] | $k_{cat}/K_m$ ($min^{-1}$ $\mu M^{-1}$) | | | |
| 14/32-mer, G | dCTP | 2 mM $Mg^{2+}$ | 112 ± 18 | 49 ± 4 | 2.3 | 1 | 1 | [118] |
| | dCTP | 0.075 mM $Mn^{2+}$ | 700 ± 40 | 0.15 ± 0.020 | 4700 | 2040 | 1 | |
| | dTTP | 2 mM $Mg^{2+}$ | 50 ± 6 | 220 ± 60 | 0.23 | 1 | $1.0 \times 10^{-1}$ | |
| | dTTP | 0.075 mM $Mn^{2+}$ | 200 ± 15 | 0.085 ± 0.020 | 2350 | 10,000 | $5.0 \times 10^{-1}$ | |
| 14/32-mer, N2-ethyl-G | dCTP | 2 mM $Mg^{2+}$ | 74 ± 12 | 36 ±3 | 2.1 | 1 | 1 | |
| | dCTP | 0.075 mM $Mn^{2+}$ | 425 ± 15 | 0.10 ± 0.012 | 4250 | 2020 | 1 | |
| | dTTP | 2 mM $Mg^{2+}$ | 115 ± 18 | 650 ± 180 | 0.18 | 1 | $8.6 \times 10^{-2}$ | |
| | dTTP | 0.075 mM $Mn^{2+}$ | 225 ± 25 | 0.030 ± 0.014 | 7500 | 41,700 | 1.7 | |

[a] Magnitude of stimulaton by Manganese was calculated as relative efficiency: $f_{rel} = (k_{cat}/K_m)_{Mn^{2+}}/(k_{cat}/K_m)_{Mg^{2+}}$. [b] Misinsertion frequency was calculated as relative efficiency: $f_{rel} = (k_{cat}/K_m)_{incorrect}/(k_{cat}/K_m)_{correct}$. [c] Steady-state kinetics: $k_{cat}$ is the turnover rate of the enzyme, $K_m$ is the Michaelis–Menten constant, and $V_{max}$ is maximum velocity of the reaction expressed as percentage of primer extended. Rows showing data measured in the presence of $Mn^{2+}$ have a blue background.

### 3.5. Polη

Like the other Y-family polymerases, Polη has low fidelity and low processivity [125,126]. Despite this, its inactivity in humans causes a UV-induced cancer-prone syndrome, which is the variant form of xeroderma pigmentosum [127]. This suggests that the major physiological function of Polη is the non-mutagenic bypass of UV lesions. Indeed, Polη has the

unique ability to efficiently and error-freely synthesize opposite CPD, which is the major UV-induced lesion [128,129]. The crystal structures of the catalytic domain of yeast and human Polη revealed that Polη has a more spacious active center than other polymerases and can accommodate cross-linked or bulky damaged bases [10,130,131]. Furthermore, structures with undamaged and damaged nucleotides are superimposable, meaning that the active site geometry is not disturbed by the lesion. This is because the catalytic domain is rigid; it acts as a molecular "splint" holding the DNA containing the lesion firmly in a stable conformation to allow for the correct base pairing and ensuing new chemical bond formation. Accordingly, Polη was shown to perform error-free or error-prone bypassing of a plethora of lesions, including 8-oxoG, [132], other oxidative damage, such as cdA [133] and 8-oxoadenine [134], AP-sites [135,136], alkylated nucleotides, such as O6mG [137,138], N7mG [48,139], N7-nitrogen half-mustard (NHMG) [140], N7-benzylguanine [141], and deaminated purines, like xanthine and hypoxanthine [140], as well as platinum adducts resulting from chemotherapy [142–144] and cross-linked peptides [145]. Additionally, Polη was shown to accommodate RNA strands for catalysis, either as a template for performing reverse transcription or as a primer for synthesizing polyribonucleotide chains or making mixed RNA-DNA strands [123,146–150]. Moreover, Polη could insert rNTPs during lesion bypassing [151]. However, rNTP incorporation by Polη is very inefficient with $Mg^{2+}$.

Besides $Mg^{2+}$, Polη can also be activated by $Mn^{2+}$ during DNA synthesis but with lower efficiency and with the price of losing base selectivity. Surprisingly, the RNA synthetic activity of Polη is greatly enhanced by $Mn^{2+}$ without significantly affecting its fidelity (Table 5) [152,153].

**Table 5.** Comparison of the effect of $Mg^{2+}$ and $Mn^{2+}$ on the catalytic activity and fidelity of yeast Polη.

| Substrate (Primer/Template), Templating Nucleotide | Incoming Nucleotide | Cation | Velocity Constant | Affinity Constant | Efficiency | Magnitude of Stimulation, $Mn^{2+}/Mg^{2+}$ [a] | Misinsertion Frequency [b] | Reference |
|---|---|---|---|---|---|---|---|---|
| | | | $k_{cat}$ ($min^{-1}$) [c] | $K_m$ (μM) [c] | $k_{cat}/K_m$ ($min^{-1}$ $\mu M^{-1}$) | | | |
| 30-mer RNA/50-mer DNA, T | rATP | 5 mM $Mg^{2+}$ | 0.24 ± 0.01 | 466± 47.3 | $5.15 \times 10^{-4}$ | 1 | | [152] |
| | rATP | 5 mM $Mn^{2+}$ | 2.61 ± 0.14 | 2.51 ± 0.64 | 1.04 | 2019 | 1 | |
| | rCTP | 5 mM $Mn^{2+}$ | 1.72 ± 0.06 | 19.4 ± 3.14 | $9 \times 10^{-2}$ | | $8.7 \times 10^{-4}$ | |
| 30-mer RNA/50-mer DNA, G | rCTP | 5 mM $Mg^{2+}$ | 2.76 ± 0.06 | 438 ± 37.5 | $6.30 \times 10^{-3}$ | 1 | | |
| | rCTP | 5 mM $Mn^{2+}$ | 4.68 ± 0.22 | 1.89 ± 0.42 | 2.48 | 394 | 1 | |
| | rGTP | 5 mM $Mn^{2+}$ | 0.31 ± 0.02 | 68.9 ± 14.9 | $4.5 \times 10^{-3}$ | | $1.8 \times 10^{-3}$ | |
| 30-mer RNA/50-mer DNA, C | rGTP | 5 mM $Mg^{2+}$ | 0.45 ± 0.01 | 394 ± 52 | $1.14 \times 10^{-3}$ | 1 | | |
| | rGTP | 5 mM $Mn^{2+}$ | 5.07 ± 0.27 | 2.55 ± 0.63 | 1.99 | 1746 | 1 | |
| | rCTP | 5 mM $Mn^{2+}$ | 1.03 ± 0.04 | 19.9 ± 3.74 | $5.2 \times 10^{-2}$ | | $2.6 \times 10^{-2}$ | |
| 30-mer RNA/50-mer DNA, A | rUTP | 5 mM $Mg^{2+}$ | 0.10 ± 0.01 | 423 ± 90.4 | $2.36 \times 10^{-4}$ | 1 | | |
| | rUTP | 5 mM $Mn^{2+}$ | 3.51 ± 0.19 | 12.8 ± 2.25 | $2.74 \times 10^{-1}$ | 1161 | 1 | |
| | rCTP | 5 mM $Mn^{2+}$ | 1.03 ± 0.07 | 17.5 ± 4.92 | $5.9 \times 10^{-2}$ | | $2.2 \times 10^{-1}$ | |
| 31-mer RNA/75-mer DNA, 8-oxoG | rCTP | 5 mM $Mg^{2+}$ | 0.034 ± 0.004 | 974 ± 270 | $3.52 \times 10^{-5}$ | 1 | | |
| | rCTP | 5 mM $Mn^{2+}$ | 0.275 ± 0.01 | 1.25 ± 0.28 | $2.20 \times 10^{-1}$ | 6286 | | |
| 13-mer RNA/29-mer DNA, TT dimer | rATP | 5 mM $Mg^{2+}$ | 0.0083 ± 0.001 | 1678 ± 445 | $4.94 \times 10^{-6}$ | 1 | | |
| | rATP | 5 mM $Mn^{2+}$ | 0.174 ± 0.005 | 11.3 ± 1.35 | $1.54 \times 10^{-2}$ | 3117 | | |

[a] Magnitude of stimulaton by Manganese was calculated as relative efficiency: $f_{rel} = (k_{cat}/K_m)_{Mn^{2+}}/(k_{cat}/K_m)_{Mg^{2+}}$. [b] Misinsertion frequency was calculated as relative efficiency: $f_{rel} = (k_{cat}/K_m)_{incorrect}/(k_{cat}/K_m)_{correct}$. [c] Steady-state kinetics: $k_{cat}$ is the turnover rate of the enzyme and $K_m$ is the Michaelis–Menten constant. Rows showing data measured in the presence of $Mn^{2+}$ have a blue background.

The optimal $Mn^{2+}$ concentration for Polη during RNA synthesis is about 5 mM, which is much higher than the physiological $Mn^{2+}$ concentration, though reduced activity could be observed below 1 mM $Mn^{2+}$. In the case of yeast Polη, $Mn^{2+}$ enhanced the incorporation of the correct rNTP 400 to 2000-fold. This increase in catalytic efficiency was due to a 2–30-

fold increase in the $k_{cat}$ and a 40–250-fold decrease in $K_m$. Importantly, the incorporation of the correct rNTPs opposite a TT dimer or 8-oxoG, which are the cognate DNA lesions of Polη, were stimulated 3000- and 6000-fold, respectively, highlighting that $Mn^{2+}$ specifically enhanced the damage bypass ability of Polη during RNA synthesis. Incorporation of the incorrect nucleotide was also enhanced somewhat, but the misincorporation frequency remained in the range of the $10^{-1}$ to $10^{-4}$ observed during DNA synthesis; therefore, fidelity was maintained. Similar results were obtained with human Polη, where $Mn^{2+}$ increased the efficiency of incorporation of the correct rNTPs 200 to 1250-fold and the correct bypass of a TT dimer and 8-oxoG 200-fold compared with $Mg^{2+}$ (Table 6) [153]. The increase was mainly due to a decreased $K_m$, while the $k_{cat}$ change was negligible. The misincorporation frequency did not change on undamaged templates and across 8-oxoG. Notably, error-free synthesis across a TT dimer became threefold more efficient than the opposite undamaged T with $Mn^{2+}$, but the fidelity was somewhat lowered. During DNA synthesis, $Mn^{2+}$ enabled Polη to replicate through difficult-to-bypass lesions. For example, in the presence of $Mg^{2+}$, the synthesis opposite cdA, which is a rigid oxidative lesion, was extremely weak, with the $k_{cat}/K_m$ being 0.015 $min^{-1}$ $\mu M^{-1}$, whilst, in the presence of $Mn^{2+}$, it almost equaled the efficiency observed opposite the undamaged A [133]. $Mn^{2+}$ enhanced the incorporation opposite the undamaged template ninefold, while it enhanced the bypass of the damage 1400-fold. This enhancement resulted from a similar increase in the affinity toward the incoming nucleotide, while the turnover rate did not change appreciably. At the same time, only the incorporation of the correct dTTP was detected, thus $Mn^{2+}$ did not compromise the fidelity of Polη. Similarly, opposite a frequent alkylated purine N7-benzylguanine (N7BnG), $Mn^{2+}$ enhanced the incorporation of the correct dCTP threefold, whereas that of the incorrect dTTP was increased fivefold; hence, the fidelity was somewhat lowered [141]. In conclusion, on one hand, $Mn^{2+}$ decreased the activity of Polη and compromised its fidelity on undamaged DNA using dNTPs, whereas it enhanced its damage bypass ability. On the other hand, it greatly increased the RNA synthetic activity of the enzyme without affecting its fidelity on undamaged DNA and promoted an even greater increase in the TLS activity during RNA synthesis.

Though the roles of Polη in HR, damage-induced sister chromatid cohesion, and transcription were described, its primary function is in the bypass of DNA lesions [154]. $Mn^{2+}$ as a metal cofactor expands the TLS activity of Polη from DNA synthesis to RNA synthesis as well.

**Table 6.** Comparison of the effect of $Mg^{2+}$ and $Mn^{2+}$ on the catalytic activity and fidelity of human Polη.

| Substrate (Primer/Template), Templating Nucleotide | Incoming Nucleotide | Cation | Velocity Constant | Affinity Constant | Efficiency | Magnitude of Stimulation, $Mn^{2+}/Mg^{2+}$ [a] | Misinsertion Frequency [b] | Reference |
|---|---|---|---|---|---|---|---|---|
| | | | $k_{cat}$ ($min^{-1}$) [c] | $K_m$ (μM) [c] | $k_{cat}/K_m$ ($min^{-1}$ $\mu M^{-1}$) | | | |
| 8-mer/11-mer, A | dTTP | 5 mM $Mg^{2+}$ | 109 ± 13 | 5.4 ± 0.7 | 20 | 1 | | [133] |
| | dTTP | $Mn^{2+}$ | 82 ± 5 | 0.44 ± 0.04 | 186 | 9.2 | | |
| 8-mer/11-mer, cdA | dTTP | 5 mM $Mg^{2+}$ | 8.6 ± 0.5 | 570 ± 70 | 0.015 | 1 | | |
| | dTTP | $Mn^{2+}$ | 10.1 ± 0.2 | 0.49 ± 0.07 | 21 | 1370 | | |
| | | | $k_{cat}$ ($10^{-3}$ $s^{-1}$) [c] | $K_m$ (μM) [c] | $k_{cat}/K_m$ ($10^{-3}$ $s^{-1}$ $\mu M^{-1}$) | | | |
| 18-mer DNA/25-mer DNA, N7BnG | dCTP | 5 mM $Mg^{2+}$ | 20.6 ± 3.6 | 10.2 ± 2.4 | 2.1 | 1 | | [141] |
| | dCTP | 1 mM $Mn^{2+}$ | 38.7 ± 4.4 | 5.6 ± 0.9 | 6.9 | 3.3 | | |
| | dTTP | 5 mM $Mg^{2+}$ | 11.5 ± 0.3 | 51.7 ± 5.3 | 0.2 | 1 | $1.0 \times 10^{-1}$ | |
| | dTTP | 1 mM $Mn^{2+}$ | 17.8 ± 2.1 | 18.6 ± 1.9 | 1.0 | 5 | $1.4 \times 10^{-1}$ | |

**Table 6.** *Cont.*

| Substrate (Primer/Template), Templating Nucleotide | Incoming Nucleotide | Cation | Velocity Constant | Affinity Constant | Efficiency | Magnitude of Stimulation, $Mn^{2+}/Mg^{2+}$ [a] | Misinsertion Frequency [b] | Reference |
|---|---|---|---|---|---|---|---|---|
| | | | $k_{cat}$ ($min^{-1}$) [c] | $K_m$ (μM) [c] | $k_{cat}/K_m$ ($min^{-1}$ $\mu M^{-1}$) | | | |
| 30-mer RNA/50-mer DNA, G | rCTP | 4 mM $Mg^{2+}$ | 0.86 ± 0.05 | 1427 ± 202 | $6.0 \times 10^{-4}$ | 1 | | [153] |
| | rCTP | 4 mM $Mn^{2+}$ | 1.27 ± 0.04 | 4.9 ± 0.6 | $2.6 \times 10^{-1}$ | 430 | 1 | |
| | rUTP | 4 mM $Mn^{2+}$ | 0.064 ± 0.004 | 995 ± 226 | $6.5 \times 10^{-5}$ | | $2.5 \times 10^{-4}$ | |
| 30-mer RNA/50-mer DNA, C | rGTP | 4 mM $Mg^{2+}$ | 0.34 ± 0.06 | 6260 ± 1564 | $5.5 \times 10^{-5}$ | 1 | | |
| | rGTP | 4 mM $Mn^{2+}$ | 0.54 ± 0.02 | 7.9 ± 0.9 | $6.9 \times 10^{-2}$ | 1260 | 1 | |
| | rUTP | 4 mM $Mn^{2+}$ | 0.030 ± 0.004 | 1274 ± 519 | $2.4 \times 10^{-5}$ | | $3.4 \times 10^{-4}$ | |
| 30-mer RNA/50-mer DNA, A | rUTP | 4 mM $Mg^{2+}$ | 0.37 ± 0.04 | 4820 ± 860 | $7.6 \times 10^{-5}$ | 1 | | |
| | rUTP | 4 mM $Mn^{2+}$ | 0.89 ± 0.03 | 5 1 ± 2.0 | $5.9 \times 10^{-2}$ | 780 | | |
| 13-mer RNA/29-mer DNA, TT dimer | rATP | 4 mM $Mg^{2+}$ | 0.54 ± 0.04 | 630 ± 124 | $8.3 \times 10^{-4}$ | 1 | | |
| | rATP | 4 mM $Mn^{2+}$ | 0.54 ± 0.02 | 3.6 ± 0.6 | $1.5 \times 10^{-1}$ | 180 | | |
| 31-mer RNA/75-mer DNA, 8-oxoG | rCTP | 4 mM $Mg^{2+}$ | 0.11 ± 0.01 | 590 ± 123 | $1.8 \times 10^{-4}$ | 1 | | |
| | rCTP | 4 mM $Mn^{2+}$ | 0.18 ± 0.01 | 4.0 ± 0.5 | $4.6 \times 10^{-2}$ | 260 | | |

[a] Magnitude of stimulaton by Manganese was calculated as relative efficiency: $f_{rel} = k_{cat}/K_m)_{Mn^{2+}} / (k_{cat}/K_m)_{Mg^{2+}}$. [b] Misinsertion frequency was calculated as relative efficiency: $f_{rel} = (k_{cat}/K_m)_{incorrect} / (k_{cat}/K_m)_{correct}$. [c] Steady-state kinetics: $k_{cat}$ is the turnover rate of the enzyme and $K_m$ is the Michaelis–Menten constant. Rows showing data measured in the presence of $Mn^{2+}$ have a blue background.

## 4. Conclusions and Future Perspectives

A small number of different DNA polymerases are available for a cell to cope with DNA lesions and DNA structure alterations that are extremely high in variety and number. Each of these so-called repair or TLS polymerases is adept at handling numerous different challenging structures, but their abilities are limited. A growing body of evidence indicates that these polymerases increase their versatility by replacing their metal cofactor $Mg^{2+}$ with $Mn^{2+}$. $Mn^{2+}$ can change the biochemical characteristics of polymerases. It can elevate or decrease the normal activity, enable lesion bypass, and change fidelity or substrate specificity; all this is undertaken to better suit the task of genome maintenance. The examples discussed above suggest that besides $Mg^{2+}$, $Mn^{2+}$ can work as a physiological metal cofactor for DNA polymerases, though supporting in vivo studies are scarce. Y and X family polymerases are not the only targets of $Mn^{2+}$. $Mn^{2+}$ was shown to enhance the activity of PrimPol, which is a recently discovered primase polymerase that belongs to the family of archaic primases and may play a role in re-priming synthesis after DNA damage (Tokarsky 2017). Furthermore, $Mn^{2+}$ is the cofactor of Mre11, which is a nuclease functioning in HR. To further support the role of $Mn^{2+}$ in DNA polymerase activation, more kinetic and thermodynamic data, as well as state-of-the-art biophysical methods, are required besides in vivo experiment. The interesting question of how the different metal cofactors are acquired by DNA polymerases remains to be answered, as well.

**Author Contributions:** Writing—original draft preparation, E.B. and I.U. All authors have read and agreed to the published version of the manuscript.

**Funding:** This research was funded by ELKH grant number PoC-2022-033.

**Conflicts of Interest:** The authors declare no conflict of interest.

## Abbreviations

| | |
|---|---|
| 8-oxoG | 8-oxoguanine |
| A | adenine |
| AP | apurinic/apyrimidinic: (abasic) |
| ATPase | adenosine-triphosphatase |
| BER | base excision repair |
| BPDE | benzo(a)pyrene diol epoxide |
| C | cytosine |
| cdA | 8:5′-cyclo-2′-deoxyadenosine |
| CPDs | cyclobutane pyrimidine dimers |
| dAMP | deoxyadenosine monophosphate |
| dATP | deoxyadenosine triphosphate |
| dCMP | deoxycytidine monophosphate |
| dCTP | deoxycytidine triphosphate |
| ddNTP | 2′3′dideoxyribonucleoside triphosphate |
| dGMP | deoxyguanosine monophosphate |
| dGTP | deoxyguanosine triphosphate |
| DNA | deoxyribonucleic acid |
| dNMP | deoxyribonucleoside monophosphate |
| dNTP | deoxyribonucleotide triphosphate |
| dRP | deoxyribophosphate |
| DSB | double-strand break |
| dTMP | deoxythymidine monophosphate |
| dTTP | deoxythymidine triphosphate |
| G | guanine |
| HR | homologous recombination |
| Mre11 | Meiotic Recombination 11 gene |
| N7BnG | N7-benzylguanine |
| N7mG | N7-methylguanine |
| NER | nucleotide excision repair |
| NHEJ | nonhomologous end-joining |
| NHMG | N7-nitrogen half-mustard |
| nt | nucleotide |
| O6mG | O6-methylguanine |
| OH | hydoxyl |
| Pol | DNA polymerase |
| rAMP | adenosine monophosphate |
| rATP | adenosine triphosphate |
| rCMP | cytidine monophosphate |
| rCTP | cytidine triphosphate |
| rGMP | guanosine monophosphate |
| rGTP | guanosine triphosphate |
| Rev1 | Reversionless 1 gene |
| RNA | ribonucleic acid |
| rNMP | ribonucleoside monophosphate |
| rNTP | ribonucleotide triphosphate |
| rUMP | uridine monophosphate |
| rUTP | uridine triphosphate |
| T | thymine |
| TdT | terminal deoxynucleotidyl transferase |
| TLS | translesion synthesis |
| U | uracil |
| V(D)J | variable: diversity and joining segments of immunoglobulin genes |

## References


1. Delagoutte, E. DNA polymerases: Mechanistic insight from biochemical and biophysical studies. *Front. Biosci.* **2012**, *17*, 509–544. [CrossRef] [PubMed]
2. Kuznetsova, A.A.; Fedorova, O.S.; Kuznetsov, N.A. Structural and Molecular Kinetic Features of Activities of DNA Polymerases. *Int. J. Mol. Sci.* **2022**, *23*, 6373. [CrossRef] [PubMed]
3. Hoitsma, N.M.; Whitaker, A.M.; Schaich, M.A.; Smith, M.R.; Fairlamb, M.S.; Freudenthal, B.D. Structure and function relationships in mammalian DNA polymerases. *Cell Mol. Life Sci.* **2020**, *77*, 35–59. [CrossRef]
4. Jain, R.; Aggarwal, A.K.; Rechkoblit, O. Eukaryotic DNA polymerases. *Curr. Opin. Struct. Biol.* **2018**, *53*, 77–87. [CrossRef]
5. Braithwaite, D.K.; Ito, J. Compilation, alignment, and phylogenetic relationships of DNA polymerases. *Nucleic Acids Res.* **1993**, *21*, 787–802. [CrossRef] [PubMed]
6. Sehnal, D.; Bittrich, S.; Deshpande, M.; Svobodová, R.; Berka, K.; Bazgier, V.; Velankar, S.; Burley, S.K.; Koča, J.; Rose, A.S. Mol* Viewer: Modern web app for 3D visualization and analysis of large biomolecular structures. *Nucleic Acids Res.* **2021**, *49*, W431–W437. [CrossRef] [PubMed]
7. Zahn, K.A.; Averill, A.M.; Aller, P.; Wood, R.D.; Doublié, S. Human DNA polymerase θ grasps the primer terminus to mediate DNA repair. *Nat. Struct. Mol. Biol.* **2015**, *22*, 304–311. [CrossRef] [PubMed]
8. Swan, M.K.; Johnson, R.E.; Prakash, L.; Prakash, S.; Aggarwal, A.K. Structural basis of high-fidelity DNA synthesis by yeast DNA polymerase δ. *Nat. Struct. Mol. Biol.* **2009**, *16*, 979–986. [CrossRef]
9. Freudenthal, B.D.; Beard, W.A.; Shock, D.D.; Wilson, S.H. Observing a DNA polymerase choose right from wrong. *Cell* **2013**, *154*, 157–168. [CrossRef]
10. Biertümpfel, C.; Zhao, Y.; Kondo, Y.; Ramón-Maiques, S.; Gregory, M.; Lee, J.Y.; Masutani, C.; Lehmann, A.R.; Hanaoka, F.; Yang, W. Structure and mechanism of human DNA polymerase η. *Nature* **2010**, *465*, 1044–1048. [CrossRef]
11. Acharya, N.; Khandagale, P.; Thakur, S.; Sahu, J.K.; Utkalaja, B.G. Quaternary structural diversity in eukaryotic DNA polymerases: Monomeric to multimeric form. *Curr. Genet.* **2020**, *66*, 635–655. [CrossRef] [PubMed]
12. Vaisman, A.; Woodgate, R. Translesion DNA polymerases in eukaryotes: What makes them tick? *Crit. Rev. Biochem. Mol. Biol.* **2017**, *52*, 274–303. [CrossRef]
13. Yang, W.; Gao, Y. Translesion and Repair DNA Polymerases: Diverse Structure and Mechanism. *Annu. Rev. Biochem.* **2018**, *87*, 239–261. [CrossRef] [PubMed]
14. Benedict, C.L.; Gilfillan, S.; Thai, T.-H.; Kearney, J.F. Terminal deoxynucleotidyl transferase and repertoire development. *Immunol. Rev.* **2000**, *175*, 150–157. [CrossRef] [PubMed]
15. Wood, R.D.; Doublié, S. DNA polymerase θ (POLQ), double-strand break repair, and cancer. *DNA Repair* **2016**, *44*, 22–32. [CrossRef]
16. Joyce, C.M.; Benkovic, S.J. DNA polymerase fidelity: Kinetics, structure, and checkpoints. *Biochemistry* **2004**, *43*, 14317–14324. [CrossRef]
17. Yang, W.; Lee, J.Y.; Nowotny, M. Making and Breaking Nucleic Acids: Two-$Mg^{2+}$-Ion Catalysis and Substrate Specificity. *Mol. Cell* **2006**, *22*, 5–13. [CrossRef]
18. Weaver, T.M.; Washington, M.T.; Freudenthal, B.D. New insights into DNA polymerase mechanisms provided by time-lapse crystallography. *Curr. Opin. Struct. Biol.* **2022**, *77*, 102465. [CrossRef]
19. Gao, Y.; Yang, W. Capture of a third Mg $^{2+}$ is essential for catalyzing DNA synthesis. *Science* **2016**, *352*, 1334–1337. [CrossRef]
20. Wang, J.; Smithline, Z.B. Crystallographic evidence for two-metal-ion catalysis in human pol η. *Protein Sci.* **2019**, *28*, 439–447. [CrossRef]
21. Tholey, G.; Ledig, M.; Mandel, P.; Sargentini, L.; Frivold, A.H.; Leroy, M.; Grippo, A.A.; Wedler, F.C. Concentrations of physiologically important metal ions in glial cells cultured from chick cerebral cortex. *Neurochem. Res.* **1988**, *13*, 45–50. [CrossRef]
22. Romani, A.; Scarpa, A. Regulation of cell magnesium. *Arch. Biochem. Biophys.* **1992**, *298*, 1–12. [CrossRef]
23. Rozenberg, J.M.; Kamynina, M.; Sorokin, M.; Zolotovskaia, M.; Koroleva, E.; Kremenchutckaya, K.; Gudkov, A.; Buzdin, A.; Borisov, N. The Role of the Metabolism of Zinc and Manganese Ions in Human Cancerogenesis. *Biomedicines* **2022**, *10*, 1072. [CrossRef]
24. Sirover, M.A.; Loeb, L.A. Metal activation of DNA synthesis. *Biochem. Biophys. Res. Commun.* **1976**, *70*, 812–817. [CrossRef]
25. Kunkel, T.A.; Loeb, L.A. On the fidelity of DNA replication. Effect of divalent metal ion activators and deoxyrionucleoside triphosphate pools on in vitro mutagenesis. *J. Biol. Chem.* **1979**, *254*, 5718–5725. [CrossRef]
26. Goodman, M.F.; Keener, S.; Guidotti, S.; Branscomb, E.W. On the enzymatic basis for mutagenesis by manganese. *J. Biol. Chem.* **1983**, *258*, 3469–3475. [CrossRef]
27. El-Deiry, W.S.; Downey, K.M.; So, A.G. Molecular mechanisms of manganese mutagenesis. *Proc. Natl. Acad. Sci. USA* **1984**, *81*, 7378–7382. [CrossRef]
28. Sawyer, D.L.; Sweasy, J.B. DNA Polymerase β in the Context of Cancer. *Crit. Rev. Oncog.* **2022**, *27*, 17–33. [CrossRef]
29. Sawaya, M.R.; Prasad, R.; Wilson, S.H.; Kraut, J.; Pelletier, H. Crystal structures of human DNA polymerase β complexed with gapped and nicked DNA: Evidence for an induced fit mechanism. *Biochemistry* **1997**, *36*, 11205–11215. [CrossRef]
30. Beard, W.A.; Wilson, S.H. Structure and mechanism of DNA polymerase β. *Biochemistry* **2014**, *53*, 2768–2780. [CrossRef]
31. Caldecott, K.W. Mammalian DNA base excision repair: Dancing in the moonlight. *DNA Repair* **2020**, *93*, 102921. [CrossRef] [PubMed]

32. Kladova, O.A.; Tyugashev, T.E.; Mikushina, E.S.; Soloviev, N.O.; Kuznetsov, N.A.; Novopashina, D.S.; Kuznetsova, A.A. Human Polβ Natural Polymorphic Variants G118V and R149I Affects Substate Binding and Catalysis. *Int. J. Mol. Sci.* **2023**, *24*, 5892. [CrossRef] [PubMed]
33. Kladova, O.A.; Fedorova, O.S.; Kuznetsov, N.A. The Role of Natural Polymorphic Variants of DNA Polymerase β in DNA Repair. *Int. J. Mol. Sci.* **2022**, *23*, 2390. [CrossRef] [PubMed]
34. Gu, H.; Marth, J.D.; Orban, P.C.; Mossmann, H.; Rajewsky, K. Deletion of a DNA polymerase β gene segment in T cells using cell type-specific gene targeting. *Science* **1994**, *265*, 103–106. [CrossRef] [PubMed]
35. Starcevic, D.; Dalal, S.; Sweasy, J.B. Is There a Link Between DNA Polymerase Beta and Cancer? *Cell Cycle* **2004**, *3*, 996–999. [CrossRef] [PubMed]
36. Donigan, K.A.; Sun, K.-W.; Nemec, A.A.; Murphy, D.L.; Cong, X.; Northrup, V.; Zelterman, D.; Sweasy, J.B. Human POLB gene is mutated in high percentage of colorectal tumors. *J. Biol. Chem.* **2012**, *287*, 23830–23839. [CrossRef] [PubMed]
37. Miller, H.; Prasad, R.; Wilson, S.H.; Johnson, F.; Grollman, A.P. 8-OxodGTP Incorporation by DNA Polymerase β Is Modified by Active-Site Residue Asn279. *Biochemistry* **2000**, *39*, 1029–1033. [CrossRef] [PubMed]
38. Kaminski, A.M.; Kunkel, T.A.; Pedersen, L.C.; Bebenek, K. Structural Insights into the Specificity of 8-Oxo-7,8-dihydro-2′-deoxyguanosine Bypass by Family X DNA Polymerases. *Genes* **2021**, *13*, 15. [CrossRef]
39. Reha-Krantz, L.J.; Nonay, R.L.; Day, R.S.; Wilson, S.H. Replication of O6-Methylguanine-containing DNA by Repair and Replicative DNA Polymerases. *J. Biol. Chem.* **1996**, *271*, 20088–20095. [CrossRef]
40. Singh, J.; Su, L.; Snow, E.T. Replication across O6-methylguanine by human dna polymerase β in vitro. *J. Biol. Chem.* **1996**, *271*, 28391–28398. [CrossRef]
41. Koag, M.-C.; Kou, Y.; Ouzon-Shubeita, H.; Lee, S. Transition-state destabilization reveals how human DNA polymerase β proceeds across the chemically unstable lesion N7-methylguanine. *Nucleic Acids Res.* **2014**, *42*, 8755–8766. [CrossRef] [PubMed]
42. Efrati, E.; Tocco, G.; Eritja, R.; Wilson, S.H.; Goodman, M.F. Abasic Translesion Synthesis by DNA Polymerase β Violates the "A-rule". *J. Biol. Chem.* **1997**, *272*, 2559–2569. [CrossRef] [PubMed]
43. Hoffmann, J.S.; Pillaire, M.J.; Maga, G.; Podust, V.; Hübscher, U.; Villani, G. DNA polymerase β bypasses in vitro a single d(GpG)-cisplatin adduct placed on codon 13 of the HRAS gene. *Proc. Natl. Acad. Sci. USA* **1995**, *92*, 5356–5360. [CrossRef]
44. Vaisman, A.; Chaney, S.G. The efficiency and fidelity of translesion synthesis past cisplatin and oxaliplatin gpg adducts by human dna polymerase β. *J. Biol. Chem.* **2000**, *275*, 13017–13025. [CrossRef] [PubMed]
45. Hoffmann, J.-S.; Pillaire, M.-J.; Garcia-Estefania, D.; Lapalu, S.; Villani, G. Bypass replication of the cisplatin-d(GPG) lesion by calf thymus dna polymerase β and human immunodeficiency virus type i reverse transcriptase is highly mutagenic. *J. Biol. Chem.* **1996**, *271*, 15386–15392. [CrossRef]
46. Vaisman, A.; Lim, S.E.; Patrick, S.M.; Copeland, W.C.; Hinkle, D.C.; Turchi, J.J.; Chaney, S.G. Effect of DNA Polymerases and High Mobility Group Protein 1 on the Carrier Ligand Specificity for Translesion Synthesis past Platinum−DNA Adducts. *Biochemistry* **1999**, *38*, 11026–11039. [CrossRef]
47. Blanca, G.; Shevelev, I.; Ramadan, K.; Villani, G.; Spadari, S.; Hübscher, U.; Maga, G. Human DNA Polymerase λ Diverged in Evolution from DNA Polymerase β toward Specific $Mn^{++}$ Dependence: A Kinetic and Thermodynamic Study. *Biochemistry* **2003**, *42*, 7467–7476. [CrossRef]
48. Koag, M.-C.; Nam, K.; Lee, S. The spontaneous replication error and the mismatch discrimination mechanisms of human DNA polymerase β. *Nucleic Acids Res.* **2014**, *42*, 11233–11245. [CrossRef]
49. Batra, V.K.; Beard, W.A.; Shock, D.D.; Pedersen, L.C.; Wilson, S.H. Structures of DNA Polymerase β with Active-Site Mismatches Suggest a Transient Abasic Site Intermediate during Misincorporation. *Mol. Cell* **2008**, *30*, 315–324. [CrossRef]
50. Beard, W.A.; Shock, D.D.; Wilson, S.H. Influence of DNA Structure on DNA Polymerase β Active Site Function. *J. Biol. Chem.* **2004**, *279*, 31921–31929. [CrossRef]
51. Pelletier, H.; Sawaya, M.R.; Wolfle, W.; Wilson, S.H.; Kraut, J. A Structural basis for metal ion mutagenicity and nucleotide selectivity in human dna polymerase β. *Biochemistry* **1996**, *35*, 12762–12777. [CrossRef] [PubMed]
52. Shtygasheva, A.A.; Belousova, E.A.; Rechkunova, N.I.; Lebedeva, N.A.; Lavrik, O.I. DNA polymerases β and λ as potential participants of TLS during genomic DNA replication on the lagging strand. *Biochemistry* **2008**, *73*, 1207–1213. [CrossRef] [PubMed]
53. Vaisman, A.; Warren, M.W.; Chaney, S.G. The Effect of DNA Structure on the Catalytic Efficiency and Fidelity of Human DNA Polymerase β on Templates with Platinum-DNA Adducts. *J. Biol. Chem.* **2001**, *276*, 18999–19005. [CrossRef] [PubMed]
54. Koag, M.-C.; Lai, L.; Lee, S. Structural Basis for the Inefficient Nucleotide Incorporation Opposite Cisplatin-DNA Lesion by Human DNA Polymerase β. *J. Biol. Chem.* **2014**, *289*, 31341–31348. [CrossRef] [PubMed]
55. Koag, M.-C.; Lee, S. Metal-Dependent Conformational Activation Explains Highly Promutagenic Replication across O6-Methylguanine by Human DNA Polymerase β. *J. Am. Chem. Soc.* **2014**, *136*, 5709–5721. [CrossRef] [PubMed]
56. Belousova, E.A.; Maga, G.; Fan, Y.; Kubareva, E.A.; Romanova, E.A.; Lebedeva, N.A.; Oretskaya, T.S.; Lavrik, O.I. DNA Polymerases β and λ Bypass Thymine Glycol in Gapped DNA Structures. *Biochemistry* **2010**, *49*, 4695–4704. [CrossRef] [PubMed]
57. Vaisman, A.; Masutani, C.; Hanaoka, F.; Chaney, S.G. Efficient translesion replication past oxaliplatin and cisplatin GPG adducts by human DNA polymerase η. *Biochemistry* **2000**, *39*, 4575–4580. [CrossRef]
58. Mentegari, E.; Kissova, M.; Bavagnoli, L.; Maga, G.; Crespan, E. DNA Polymerases λ and β: The Double-Edged Swords of DNA Repair. *Genes* **2016**, *7*, 57. [CrossRef]

59. van Loon, B.; Hübscher, U.; Maga, G. Living on the Edge: DNA Polymerase Lambda between Genome Stability and Mutagenesis. *Chem. Res. Toxicol.* **2017**, *30*, 1936–1941. [CrossRef]
60. Garcia-Diaz, M.; Domínguez, O.; López-Fernández, L.A.; de Lera, L.T.; Saníger, M.L.; Ruiz, J.F.; Párraga, M.; García-Ortiz, M.J.; Kirchhoff, T.; del Mazo, J.; et al. DNA polymerase lambda (Pol λ), a novel eukaryotic DNA polymerase with a potential role in meiosis. *J. Mol. Biol.* **2000**, *301*, 851–867. [CrossRef]
61. García-Díaz, M.; Bebenek, K.; Kunkel, T.A.; Blanco, L. Identification of an Intrinsic 5′-Deoxyribose-5-phosphate Lyase Activity in Human DNA Polymerase λ. *J. Biol. Chem.* **2001**, *276*, 34659–34663. [CrossRef]
62. Ramadan, K.; Shevelev, I.V.; Maga, G.; Hübscher, U. De Novo DNA Synthesis by Human DNA Polymerase λ, DNA Polymerase μ and Terminal Deoxyribonucleotidyl Transferase. *J. Mol. Biol.* **2004**, *339*, 395–404. [CrossRef]
63. Garcia-Diaz, M.; Bebenek, K.; Krahn, J.M.; Kunkel, T.A.; Pedersen, L.C. A closed conformation for the Pol λ catalytic cycle. *Nat. Struct. Mol. Biol.* **2005**, *12*, 97–98. [CrossRef]
64. Picher, A.J. Promiscuous mismatch extension by human DNA polymerase lambda. *Nucleic Acids Res.* **2006**, *34*, 3259–3266. [CrossRef]
65. Liu, M.-S.; Tsai, H.-Y.; Liu, X.-X.; Ho, M.-C.; Wu, W.-J.; Tsai, M.-D. Structural Mechanism for the Fidelity Modulation of DNA Polymerase λ. *J. Am. Chem. Soc.* **2016**, *138*, 2389–2398. [CrossRef]
66. Bebenek, K.; Garcia-Diaz, M.; Blanco, L.; Kunkel, T.A. The Frameshift Infidelity of Human DNA Polymerase λ. *J. Biol. Chem.* **2003**, *278*, 34685–34690. [CrossRef]
67. Brown, J.A.; Pack, L.R.; Sanman, L.E.; Suo, Z. Efficiency and fidelity of human DNA polymerases λ and β during gap-filling DNA synthesis. *DNA Repair* **2011**, *10*, 24–33. [CrossRef]
68. Braithwaite, E.K.; Kedar, P.S.; Stumpo, D.J.; Bertocci, B.; Freedman, J.H.; Samson, L.D.; Wilson, S.H. DNA polymerases β and λ mediate overlapping and independent roles in base excision repair in mouse embryonic fibroblasts. *PLoS ONE* **2010**, *5*, e12229. [CrossRef]
69. Lee, J.W.; Blanco, L.; Zhou, T.; Garcia-Diaz, M.; Bebenek, K.; Kunkel, T.A.; Wang, Z.; Povirk, L.F. Implication of DNA Polymerase λ in Alignment-based Gap Filling for Nonhomologous DNA End Joining in Human Nuclear Extracts. *J. Biol. Chem.* **2004**, *279*, 805–811. [CrossRef]
70. Belousova, E.; Lavrik, O. DNA polymerases β and λ and their roles in Cell DNA Repair 2015, 29, 112–126. *DNA Repair* **2015**, *29*, 112–126. [CrossRef]
71. Pryor, J.M.; Waters, C.A.; Aza, A.; Asagoshi, K.; Strom, C.; Mieczkowski, P.A.; Blanco, L.; Ramsden, D.A. Essential role for polymerase specialization in cellular nonhomologous end joining. *Proc. Natl. Acad. Sci. USA* **2015**, *112*, E4537–E4545. [CrossRef]
72. Ramadan, K.; Shevelev, I.V.; Maga, G.; Hübscher, U. DNA Polymerase λ from Calf Thymus Preferentially Replicates Damaged DNA. *J. Biol. Chem.* **2002**, *277*, 18454–18458. [CrossRef]
73. Maga, G.; Villani, G.; Crespan, E.; Wimmer, U.; Ferrari, E.; Bertocci, B.; Hübscher, U. 8-oxo-guanine bypass by human DNA polymerases in the presence of auxiliary proteins. *Nature* **2007**, *447*, 606–608. [CrossRef]
74. Picher, A.J.; Blanco, L. Human DNA polymerase lambda is a proficient extender of primer ends paired to 7,8-dihydro-8-oxoguanine. *DNA Repair* **2007**, *6*, 1749–1756. [CrossRef]
75. Brown, J.A.; Duym, W.W.; Fowler, J.D.; Suo, Z. Single-turnover Kinetic Analysis of the Mutagenic Potential of 8-Oxo-7,8-dihydro-2′-deoxyguanosine during Gap-filling Synthesis Catalyzed by Human DNA Polymerases λ and β. *J. Mol. Biol.* **2007**, *367*, 1258–1269. [CrossRef]
76. Crespan, E.; Hübscher, U.; Maga, G. Error-free bypass of 2-hydroxyadenine by human DNA polymerase with Proliferating Cell Nuclear Antigen and Replication Protein A in different sequence contexts. *Nucleic Acids Res.* **2007**, *35*, 5173–5181. [CrossRef]
77. Yoon, J.-H.; Basu, D.; Sellamuthu, K.; Johnson, R.E.; Prakash, S.; Prakash, L. A novel role of DNA polymerase λ in translesion synthesis in conjunction with DNA polymerase ζ. *Life Sci. Alliance* **2021**, *4*, e202000900. [CrossRef]
78. Yoon, J.-H.; Basu, D.; Choudhury, J.R.; Prakash, S.; Prakash, L. DNA polymerase λ promotes error-free replication through Watson–Crick impairing N1-methyl-deoxyadenosine adduct in conjunction with DNA polymerase ζ. *J. Biol. Chem.* **2021**, *297*, 100868. [CrossRef]
79. Maga, G. Human replication protein A can suppress the intrinsic in vitro mutator phenotype of human DNA polymerase. *Nucleic Acids Res.* **2006**, *34*, 1405–1415. [CrossRef]
80. Bertocci, B.; De Smet, A.; Berek, C.; Weill, J.-C.; Reynaud, C.-A. Immunoglobulin κ Light Chain Gene Rearrangement Is Impaired in Mice Deficient for DNA Polymerase Mu. *Immunity* **2003**, *19*, 203–211. [CrossRef]
81. Bertocci, B.; De Smet, A.; Weill, J.-C.; Reynaud, C.-A. Nonoverlapping Functions of DNA Polymerases Mu, Lambda, and Terminal Deoxynucleotidyltransferase during Immunoglobulin V(D)J Recombination In Vivo. *Immunity* **2006**, *25*, 31–41. [CrossRef]
82. McElhinny, S.A.N.; Havener, J.M.; Garcia-Diaz, M.; Juárez, R.; Bebenek, K.; Kee, B.L.; Blanco, L.; Kunkel, T.A.; Ramsden, D.A. A Gradient of Template Dependence Defines Distinct Biological Roles for Family X Polymerases in Nonhomologous End Joining. *Mol. Cell* **2005**, *19*, 357–366. [CrossRef]
83. Ghosh, D.; Raghavan, S.C. 20 years of DNA Polymerase μ, the polymerase that still surprises. *FEBS J.* **2021**, *288*, 7230–7242. [CrossRef]
84. Domínguez, O.; Ruiz, J.F.; de Lera, T.L.; García-Díaz, M.; González, M.A.; Kirchhoff, T.; Martínez-A, C.; Bernad, A.; Blanco, L. DNA polymerase mu (Pol micro), homologous to TdT, could act as a DNA mutator in eukaryotic cells. *EMBO J.* **2000**, *19*, 1731–1742. [CrossRef]

85. Juárez, R.; Ruiz, J.F.; McElhinny, S.A.N.; Ramsden, D.; Blanco, L. A specific loop in human DNA polymerase mu allows switching between creative and DNA-instructed synthesis. *Nucleic Acids Res.* **2006**, *34*, 4572–4582. [CrossRef]
86. Zhang, Y.; Wu, X.; Yuan, F.; Xie, Z.; Wang, Z. Highly Frequent Frameshift DNA Synthesis by Human DNA Polymerase μ. *Mol. Cell Biol.* **2001**, *21*, 7995–8006. [CrossRef]
87. Moon, A.F.; Gosavi, R.A.; Kunkel, T.A.; Pedersen, L.C.; Bebenek, K. Creative template-dependent synthesis by human polymerase mu. *Proc. Natl. Acad. Sci. USA* **2015**, *112*, E4530–E4536. [CrossRef]
88. Moon, A.F.; Pryor, J.M.; Ramsden, D.A.; Kunkel, T.A.; Bebenek, K.; Pedersen, L.C. Sustained active site rigidity during synthesis by human DNA polymerase μ. *Nat. Struct. Mol. Biol.* **2014**, *21*, 253–260. [CrossRef]
89. Ruiz, J.F. Lack of sugar discrimination by human Pol requires a single glycine residue. *Nucleic Acids Res.* **2003**, *31*, 4441–4449. [CrossRef]
90. McElhinny, S.A.N.; Ramsden, D.A. Polymerase Mu Is a DNA-Directed DNA/RNA Polymerase. *Mol. Cell Biol.* **2003**, *23*, 2309–2315. [CrossRef]
91. Moon, A.F.; Pryor, J.M.; Ramsden, D.A.; Kunkel, T.A.; Bebenek, K.; Pedersen, L.C. Structural accommodation of ribonucleotide incorporation by the DNA repair enzyme polymerase Mu. *Nucleic Acids Res.* **2017**, *45*, 9138–9148. [CrossRef]
92. Zhang, Y.; Wu, X.; Guo, D.; Rechkoblit, O.; Taylor, J.-S.; Geacintov, N.E.; Wang, Z. Lesion bypass activities of human DNA polymerase μ. *J. Biol. Chem.* **2002**, *277*, 44582–44587. [CrossRef]
93. Havener, J.M.; McElhinny, S.A.N.; Bassett, E.; Gauger, M.; Ramsden, D.A.; Chaney, S.G. Translesion synthesis past platinum DNA adducts by human DNA polymerase μ. *Biochemistry* **2003**, *42*, 1777–1788. [CrossRef]
94. Kaminski, A.M.; Chiruvella, K.K.; Ramsden, D.A.; Kunkel, T.A.; Bebenek, K.; Pedersen, L.C. Unexpected behavior of DNA polymerase Mu opposite template 8-oxo-7,8-dihydro-2′-guanosine. *Nucleic Acids Res.* **2019**, *47*, 9410–9422. [CrossRef]
95. Martin, M.J.; Garcia-Ortiz, M.V.; Esteban, V.; Blanco, L. Ribonucleotides and manganese ions improve non-homologous end joining by human Polμ. *Nucleic Acids Res.* **2013**, *41*, 2428–2436. [CrossRef]
96. Jamsen, J.A.; Beard, W.A.; Pedersen, L.C.; Shock, D.D.; Moon, A.F.; Krahn, J.M.; Bebenek, K.; Kunkel, T.A.; Wilson, S.H. Time-lapse crystallography snapshots of a double-strand break repair polymerase in action. *Nat. Commun.* **2017**, *8*, 253. [CrossRef]
97. Jamsen, J.A.; Sassa, A.; Perera, L.; Shock, D.D.; Beard, W.A.; Wilson, S.H. Structural basis for proficient oxidized ribonucleotide insertion in double strand break repair. *Nat. Commun.* **2021**, *12*, 5055. [CrossRef]
98. Jamsen, J.A.; Sassa, A.; Shock, D.D.; Beard, W.A.; Wilson, S.H. Watching a double strand break repair polymerase insert a pro-mutagenic oxidized nucleotide. *Nat. Commun.* **2021**, *12*, 2059. [CrossRef]
99. Guo, M.; Wang, Y.; Tang, Y.; Chen, Z.; Hou, J.; Dai, J.; Wang, Y.; Wang, L.; Xu, H.; Tian, B.; et al. Mechanism of genome instability mediated by human DNA polymerase mu misincorporation. *Nat. Commun.* **2021**, *12*, 1–9. [CrossRef]
100. Chang, Y.-K.; Huang, Y.-P.; Liu, X.-X.; Ko, T.-P.; Bessho, Y.; Kawano, Y.; Maestre-Reyna, M.; Wu, W.-J.; Tsai, M.-D. Human DNA Polymerase μ Can Use a Noncanonical Mechanism for Multiple $Mn^{2+}$-Mediated Functions. *J. Am. Chem. Soc.* **2019**, *141*, 8489–8502. [CrossRef] [PubMed]
101. Pryor, J.M.; Conlin, M.P.; Carvajal-Garcia, J.; Luedeman, M.E.; Luthman, A.J.; Small, G.W.; Ramsden, D.A. Ribonucleotide incorporation enables repair of chromosome breaks by nonhomologous end joining. *Science* **2018**, *361*, 1126–1129. [CrossRef] [PubMed]
102. Çağlayan, M. Pol μ ribonucleotide insertion opposite 8-oxodG facilitates the ligation of premutagenic DNA repair intermediate. *Sci. Rep.* **2020**, *10*, 1–14. [CrossRef]
103. McIntyre, J. Polymerase iota—An odd sibling among Y family polymerases. *DNA Repair* **2020**, *86*, 102753. [CrossRef] [PubMed]
104. Bebenek, K.; Tissier, A.; Frank, E.G.; McDonald, J.P.; Prasad, R.; Wilson, S.H.; Woodgate, R.; Kunkel, T.A. 5′-Deoxyribose Phosphate lyase activity of human DNA polymerase ι in vitro. *Science* **2001**, *291*, 2156–2159. [CrossRef] [PubMed]
105. Tissier, A.; McDonald, J.P.; Frank, E.G.; Woodgate, R. polι, a remarkably error-prone human DNA polymerase. *Minerva Anestesiol.* **2000**, *14*, 1642–1650. [CrossRef]
106. Johnson, R.E.; Washington, M.T.; Haracska, L.; Prakash, S.; Prakash, L. Eukaryotic polymerases ι and ζ act sequentially to bypass DNA lesions. *Nature* **2000**, *406*, 1015–1019. [CrossRef] [PubMed]
107. Zhang, Y.; Yuan, F.; Wu, X.; Wang, Z. Preferential Incorporation of G Opposite Template T by the Low-Fidelity Human DNA Polymerase ι. *Mol. Cell Biol.* **2000**, *20*, 7099–7108. [CrossRef]
108. Nair, D.T.; Johnson, R.E.; Prakash, S.; Prakash, L.; Aggarwal, A.K. Replication by human DNA polymerase-ι occurs by Hoogsteen base-pairing. *Nature* **2004**, *430*, 377–380. [CrossRef]
109. Choi, J.-Y.; Lim, S.; Eoff, R.L.; Guengerich, F.P. Kinetic Analysis of Base-Pairing Preference for Nucleotide Incorporation Opposite Template Pyrimidines by Human DNA Polymerase ι. *J. Mol. Biol.* **2009**, *389*, 264–274. [CrossRef]
110. Zhang, Y. Response of human DNA polymerase iota to DNA lesions. *Nucleic Acids Res.* **2001**, *29*, 928–935. [CrossRef]
111. Tissier, A.; Frank, E.G.; McDonald, J.P.; Iwai, S.; Hanaoka, F.; Woodgate, R. Misinsertion and bypass of thymine–thymine dimers by human DNA polymerase ι. *EMBO J.* **2000**, *19*, 5259–5266. [CrossRef] [PubMed]
112. Jain, R.; Choudhury, J.R.; Buku, A.; Johnson, R.E.; Prakash, L.; Prakash, S.; Aggarwal, A.K. Mechanism of error-free DNA synthesis across N1-methyl-deoxyadenosine by human DNA polymerase-ι. *Sci. Rep.* **2017**, *7*, 43904. [CrossRef] [PubMed]
113. Plosky, B.S.; Frank, E.G.; Berry, D.A.; Vennall, G.P.; McDonald, J.P.; Woodgate, R. Eukaryotic Y-family polymerases bypass a 3-methyl-2′-deoxyadenosine analog in vitro and methyl methanesulfonate-induced DNA damage in vivo. *Nucleic Acids Res.* **2008**, *36*, 2152–2162. [CrossRef] [PubMed]

114. Yoon, J.-H.; Choudhury, J.R.; Park, J.; Prakash, S.; Prakash, L. Translesion synthesis DNA polymerases promote error-free replication through the minor-groove DNA adduct 3-deaza-3-methyladenine. *J. Biol. Chem.* **2017**, *292*, 18682–18688. [CrossRef] [PubMed]
115. Yoon, J.-H.; Choudhury, J.R.; Prakash, L.; Prakash, S. Translesion synthesis DNA polymerases η, ι, and ν promote mutagenic replication through the anticancer nucleoside cytarabine. *J. Biol. Chem.* **2019**, *294*, 19048–19054. [CrossRef] [PubMed]
116. Frank, E.G.; Woodgate, R. Increased catalytic activity and altered fidelity of human DNA polymerase ι in the presence of manganese. *J. Biol. Chem.* **2007**, *282*, 24689–24696. [CrossRef] [PubMed]
117. Donigan, K.A.; McLenigan, M.P.; Yang, W.; Goodman, M.F.; Woodgate, R. The Steric Gate of DNA Polymerase ι Regulates Ribonucleotide Incorporation and Deoxyribonucleotide Fidelity. *J. Biol. Chem.* **2014**, *289*, 9136–9145. [CrossRef]
118. Pence, M.G.; Blans, P.; Zink, C.N.; Hollis, T.; Fishbein, J.C.; Perrino, F.W. Lesion bypass of N2-ethylguanine by human DNA polymerase ι. *J. Biol. Chem.* **2009**, *284*, 1732–1740. [CrossRef]
119. Poltoratsky, V.; Woo, C.J.; Tippin, B.; Martin, A.; Goodman, M.F.; Scharff, M.D. Expression of error-prone polymerases in BL2 cells activated for Ig somatic hypermutation. *Proc. Natl. Acad. Sci. USA* **2001**, *98*, 7976–7981. [CrossRef]
120. Faili, A.; Aoufouchi, S.; Flatter, E.; Guéranger, Q.; Reynaud, C.-A.; Weill, J.-C. Induction of somatic hypermutation in immunoglobulin genes is dependent on DNA polymerase iota. *Nature* **2002**, *419*, 944–947. [CrossRef]
121. McDonald, J.P.; Frank, E.G.; Plosky, B.S.; Rogozin, I.B.; Masutani, C.; Hanaoka, F.; Woodgate, R.; Gearhart, P.J. 129-Derived strains of mice are deficient in DNA polymerase ι and have normal immunoglobulin hypermutation. *J. Exp. Med.* **2003**, *198*, 635–643. [CrossRef] [PubMed]
122. Shimizu, T.; Azuma, T.; Ishiguro, M.; Kanjo, N.; Yamada, S.; Ohmori, H. Normal immunoglobulin gene somatic hypermutation in Polκ–Polι double-deficient mice. *Immunol. Lett.* **2005**, *98*, 259–264. [CrossRef] [PubMed]
123. Gueranger, Q.; Stary, A.; Aoufouchi, S.; Faili, A.; Sarasin, A.; Reynaud, C.-A.; Weill, J.-C. Role of DNA polymerases η, ι and ζ in UV resistance and UV-induced mutagenesis in a human cell line. *DNA Repair* **2008**, *7*, 1551–1562. [CrossRef] [PubMed]
124. Ziv, O.; Geacintov, N.; Nakajima, S.; Yasui, A.; Livneh, Z. DNA polymerase ζ cooperates with polymerases κ and ι in translesion DNA synthesis across pyrimidine photodimers in cells from XPV patients. *Proc. Natl. Acad. Sci. USA* **2009**, *106*, 11552–11557. [CrossRef] [PubMed]
125. Johnson, R.E.; Washington, M.T.; Prakash, S.; Prakash, L. Fidelity of human DNA polymerase η. *J. Biol. Chem.* **2000**, *275*, 7447–7450. [CrossRef] [PubMed]
126. Washington, M.T.; Johnson, R.E.; Prakash, S.; Prakash, L. Fidelity and processivity of saccharomyces cerevisiae DNA polymerase η. *J. Biol. Chem.* **1999**, *274*, 36835–36838. [CrossRef] [PubMed]
127. Feltes, B.C.; Menck, C.F.M. Current state of knowledge of human DNA polymerase eta protein structure and disease-causing mutations. *Mutat. Res. Mol. Mech. Mutagen.* **2022**, *790*, 108436. [CrossRef] [PubMed]
128. Johnson, R.E.; Prakash, S.; Prakash, L. Efficient bypass of a thymine-thymine dimer by yeast DNA polymerase, polη. *Science* **1999**, *283*, 1001–1004. [CrossRef]
129. Washington, M.T.; Johnson, R.E.; Prakash, S.; Prakash, L. Accuracy of thymine-thymine dimer bypass by Saccharomyces cerevisiae DNA polymerase η. *Proc. Natl. Acad. Sci. USA* **2000**, *97*, 3094–3099. [CrossRef]
130. Trincao, J.; Johnson, R.E.; Escalante, C.R.; Prakash, S.; Prakash, L.; Aggarwal, A.K. Structure of the Catalytic Core of S. cerevisiae DNA Polymerase η: Implications for Translesion DNA Synthesis. *Mol. Cell* **2001**, *8*, 417–426. [CrossRef]
131. Silverstein, T.D.; Jain, R.; Johnson, R.E.; Prakash, L.; Prakash, S.; Aggarwal, A.K. Structural Basis for Error-free Replication of Oxidatively Damaged DNA by Yeast DNA Polymerase η. *Structure* **2010**, *18*, 1463–1470. [CrossRef] [PubMed]
132. Haracska, L.; Yu, S.-L.; Johnson, R.E.; Prakash, L.; Prakash, S. Efficient and accurate replication in the presence of 7,8-dihydro-8-oxoguanine by DNA polymerase η. *Nat. Genet.* **2000**, *25*, 458–461. [CrossRef] [PubMed]
133. Weng, P.J.; Gao, Y.; Gregory, M.T.; Wang, P.; Wang, Y.; Yang, W. Bypassing a 8,5′-cyclo-2′-deoxyadenosine lesion by human DNA polymerase η at atomic resolution. *Proc. Natl. Acad. Sci. USA* **2018**, *115*, 10660–10665. [CrossRef] [PubMed]
134. Koag, M.-C.; Jung, H.; Lee, S. Mutagenesis mechanism of the major oxidative adenine lesion 7,8-dihydro-8-oxoadenine. *Nucleic Acids Res.* **2020**, *48*, 5119–5134. [CrossRef]
135. Haracska, L.; Washington, M.T.; Prakash, S.; Prakash, L. Inefficient Bypass of an Abasic Site by DNA Polymerase η. *J. Biol. Chem.* **2001**, *276*, 6861–6866. [CrossRef]
136. Patra, A.; Zhang, Q.; Lei, L.; Su, Y.; Egli, M.; Guengerich, F.P. Structural and kinetic analysis of nucleoside triphosphate incorporation opposite an abasic site by human translesion DNA polymerase η. *J. Biol. Chem.* **2015**, *290*, 8028–8038. [CrossRef]
137. Haracska, L.; Prakash, S.; Prakash, L. Replication past $O^6$-Methylguanine by Yeast and Human DNA Polymerase η. *Mol. Cell Biol.* **2000**, *20*, 8001–8007. [CrossRef]
138. Patra, A.; Zhang, Q.; Guengerich, F.P.; Egli, M. Mechanisms of insertion of dCTP and dTTP opposite the DNA lesion O6-Methyl-26-deoxyguanosine by Human DNA polymerase η. *J. Biol. Chem.* **2016**, *291*, 24304–24313. [CrossRef]
139. Koag, M.-C.; Jung, H.; Kou, Y.; Lee, S. Bypass of the major alkylative DNA lesion by human DNA polymerase η. *Molecules* **2019**, *24*, 3928. [CrossRef]
140. Jung, H.; Hawkins, M.A.; Lee, S. Structural insights into the bypass of the major deaminated purines by translesion synthesis DNA polymerase. *Biochem. J.* **2020**, *477*, 4797–4810. [CrossRef]
141. Jung, H.; Rayala, N.K.; Lee, S. Effects of N7-Alkylguanine Conformation and Metal Cofactors on the Translesion Synthesis by Human DNA Polymerase η. *Chem. Res. Toxicol.* **2022**, *35*, 512–521. [CrossRef] [PubMed]

142. Zhao, Y.; Biertümpfel, C.; Gregory, M.T.; Hua, Y.-J.; Hanaoka, F.; Yang, W. Structural basis of human DNA polymerase η-mediated chemoresistance to cisplatin. *Proc. Natl. Acad. Sci. USA* **2012**, *109*, 7269–7274. [CrossRef] [PubMed]
143. Gregory, M.T.; Park, G.Y.; Johnstone, T.C.; Lee, Y.-S.; Yang, W.; Lippard, S.J. Structural and mechanistic studies of polymerase η bypass of phenanthriplatin DNA damage. *Proc. Natl. Acad. Sci. USA* **2014**, *111*, 9133–9138. [CrossRef] [PubMed]
144. Ouzon-Shubeita, H.; Baker, M.; Koag, M.-C.; Lee, S. Structural basis for the bypass of the major oxaliplatin–DNA adducts by human DNA polymerase η. *Biochem. J.* **2019**, *476*, 747–758. [CrossRef] [PubMed]
145. Ghodke, P.P.; Guengerich, F.P. DNA polymerases η and κ bypass N2-guanine-O6-alkylguanine DNA alkyltransferase cross-linked DNA-peptides. *J. Biol. Chem.* **2021**, *297*, 101124. [CrossRef] [PubMed]
146. Su, Y.; Egli, M.; Guengerich, F.P. Mechanism of Ribonucleotide Incorporation by Human DNA Polymerase η. *J. Biol. Chem.* **2016**, *291*, 3747–3756. [CrossRef] [PubMed]
147. Gali, V.K.; Balint, E.; Serbyn, N.; Frittmann, O.; Stutz, F.; Unk, I. Translesion synthesis DNA polymerase η exhibits a specific RNA extension activity and a transcription-associated function. *Sci. Rep.* **2017**, *7*, 13055. [CrossRef] [PubMed]
148. Sassa, A.; Çağlayan, M.; Rodriguez, Y.; Beard, W.A.; Wilson, S.H.; Nohmi, T.; Honma, M.; Yasui, M. Impact of ribonucleotide backbone on translesion synthesis and repair of 7,8-Dihydro-8-oxoguanine. *J. Biol. Chem.* **2016**, *291*, 24314–24323. [CrossRef]
149. Su, Y.; Ghodke, P.P.; Egli, M.; Li, L.; Wang, Y.; Guengerich, F.P. Human DNA polymerase η has reverse transcriptase activity in cellular environments. *J. Biol. Chem.* **2019**, *294*, 6073–6081. [CrossRef]
150. Su, Y.; Egli, M.; Guengerich, F.P. Human DNA polymerase η accommodates RNA for strand extension. *J. Biol. Chem.* **2017**, *292*, 18044–18051. [CrossRef]
151. Mentegari, E.; Crespan, E.; Bavagnoli, L.; Kissova, M.; Bertoletti, F.; Sabbioneda, S.; Imhof, R.; Sturla, S.J.; Nilforoushan, A.; Hübscher, U.; et al. Ribonucleotide incorporation by human DNA polymerase η impacts translesion synthesis and RNase H2 activity. *Nucleic Acids Res.* **2017**, *45*, 2600–2614. [CrossRef] [PubMed]
152. Balint, E.; Unk, I. Selective Metal Ion Utilization Contributes to the Transformation of the Activity of Yeast Polymerase η from DNA Polymerization toward RNA Polymerization. *Int. J. Mol. Sci.* **2020**, *21*, 8248. [CrossRef] [PubMed]
153. Balint, E.; Unk, I. Manganese is a strong specific activator of the RNA synthetic activity of human polη. *Int. J. Mol. Sci.* **2022**, *23*, 230. [CrossRef] [PubMed]
154. Acharya, N.; Manohar, K.; Peroumal, D.; Khandagale, P.; Patel, S.K.; Sahu, S.R.; Kumari, P. Multifaceted activities of DNA polymerase η: Beyond translesion DNA synthesis. *Curr. Genet.* **2018**, *65*, 649–656. [CrossRef]